

Positional Bias in Long-Document Ranking: Impact, Assessment, and Mitigation

Anonymous ACL submission

Abstract

We tested over 20 Transformer models for ranking of long documents (including recent *LongP* models trained with FlashAttention and RankGPT models “powered” by OpenAI and Anthropic cloud APIs). We compared them with a simple *FirstP* baselines, which applied the *same* model to the truncated input (at most 512 tokens). On MS MARCO, TREC DL, and Robust04 no long-document model outperformed *FirstP* by more than 5% (on average). We hypothesized that the lack of improvement by long-context models is not due to inherent model limitations, but due to benchmark positional bias (most relevant passages tend to occur early in documents), **which is known to exist in MS MARCO**. To further confirm this we analyzed positional relevance distributions across five corpora and six query sets and observed the same early-position bias. We then introduced a new diagnostic dataset, MS MARCO FarRelevant, where relevant spans were deliberately placed beyond the first 512 tokens. On this dataset, many long-context models—including RankGPT—failed to generalize and performed near the random baseline, suggesting overfitting to positional bias. Finally, we experimented with de-biasing the training data, but the success of this approach was mixed. Our findings (1) highlight the need for careful benchmark design in evaluating long-context models for document ranking, (2) identify model types that are more robust to positional bias, and (3) motivate further work on approaches to de-bias training data. We release our code and data to support further research.¹

1 Introduction

Various advances in Transformer architectures—including sparse attention (Zaheer et al., 2020; Beltagy et al., 2020) and FlashAttention (Dao et al.,

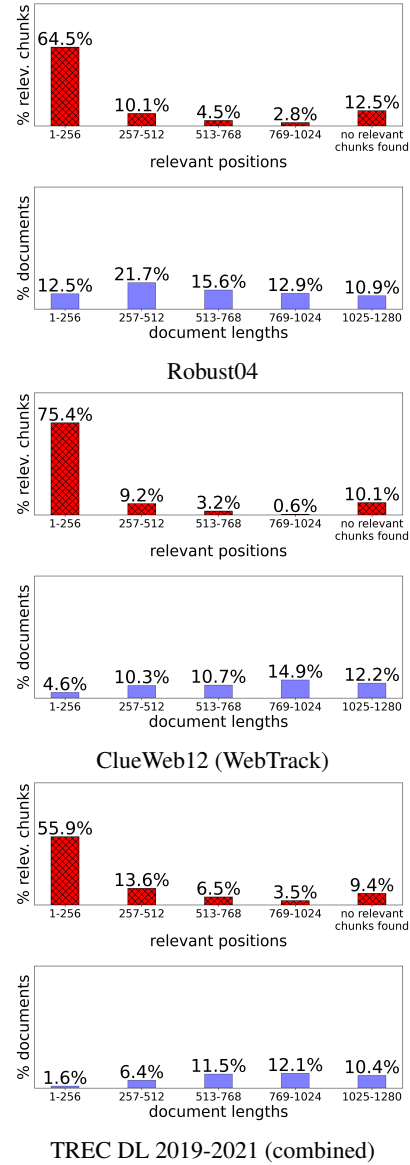


Figure 1: **Illustration of positional relevance bias for three document collections.** We show a distribution of first relevant passage positions (red bars) vs. relevant document lengths (blue bars). Lengths and offsets are measured in the number of subword tokens (BERT-base tokenizer). Best viewed in color. See more results in Table 7 in § B.1

¹https://anonymous.4open.science/r/long_doc_rank_model_analysis_v2-78E9/.

2022)—have motivated a growing interest in long-document ranking and retrieval. However, despite the ability of these models to process substantially more text, on *popular retrieval benchmarks*, the improvements of these models over simpler truncation-based approaches remain surprisingly modest (Dai and Callan, 2019; Gao and Callan, 2022; Coelho et al., 2024). A widely used truncation-based *FirstP* baseline (Dai and Callan, 2019)—where models score only the first 512 tokens of each document—often performs competitively, or sometimes even better, than long-context counterparts (see, e.g., Table 1).

Despite anecdotal knowledge about the presence of this phenomenon in the MS MARCO document-retrieval collection among TREC Deep Learning track participants and some early reports (Hofstätter et al., 2020b, 2021a) the available evidence has been scattered and incomplete. In particular, despite the track’s five-year history, none of the track’s overview papers mentioned this issue (Craswell et al., 2020, 2021a,b, 2022, 2023).

Moreover, it remains unclear whether these limitations stem from model deficiencies or from characteristics of the benchmarks themselves. In this paper, we initially hypothesized that both factors—model robustness and benchmark design—may be responsible for the limited gains of long-document models over *FirstP* baselines. However, our findings suggest that benchmark design, particularly positional relevance bias, is the dominating factor.

To verify our research hypotheses, we first conducted a large-scale, systematic study of over 20 Transformer-based ranking models (Devlin et al., 2019; Vaswani et al., 2017) for long-document retrieval. This was done using three popular document collections—MS MARCO Documents v1/v2 (Craswell et al., 2021a) and Robust04 (Clarke et al., 2004)—along with diverse query sets (both large and small) several Transformer backbones and multiple training seeds. In addition to locally trained models, we also assessed a listwise LLM ranker RankGPT (Sun et al., 2023) “powered” by OpenAI (OpenAI, 2023) and Anthropic (Anthropic, 2024) cloud APIs. Despite the increased context capacity of long-document models, we found that none of them consistently outperformed their *FirstP* baselines by more than 5% on average.

Next, we estimated positional relevance bias across five document collections (including MS

MARCO v2) and more than six query sets. As can be seen in Fig. 1, in the vast majority of cases the first relevant passage occurred within the initial 512 tokens. In contrast, the distribution of *relevant* passage positions is more uniform and has a long tail. This confirms the presence of positional bias not only in MS MARCO, but also in other TREC collections (a complete set of plots is provided in Fig. 7 of Appendix § B.4).

Our initial exploration prompted two *broad* research questions:

- **RQ1:** How robust are long-document models to the positional-bias of relevant passages?
- **RQ2:** To what extent has the research community advanced the state of long-document ranking models? Specifically, do current approaches yield substantial improvements over *FirstP* baselines? Considering that all existing long-document models are at least 2× slower than their respective *FirstP* counterparts (see Figure 3, § A.4), it is reasonable to question the practicality of such models and to consider whether *FirstP* variants might be preferable in real-world applications.

To answer these questions, we constructed a new *diagnostic* synthetic collection MS MARCO Far-Relevant where relevant passages were not present among the first 512 tokens. On this dataset, many long-context models—including RankGPT (Sun et al., 2023)—failed to generalize and performed at a random baseline level, suggesting overfitting to positional bias. Poor performance of several models on our new synthetic collection prompted another important question **RQ3:** Can de-biasing training data mitigate model overfitting to positional bias? We addressed this question by evaluating an existing de-biasing approach (Hofstätter et al., 2021a).

Our paper makes the following contributions:

- We re-examined the issue of positional relevance bias, gathered extensive evidence confirming its presence in several datasets, showed that it negatively affects all models including recent LLM-based rankers, and evaluated the robustness of ranking models against this bias using a new diagnostic dataset MS MARCO FarRelevant.
- Our work highlights the need for careful benchmark design in evaluating long-context

models for document ranking, which do not mask the benefits of long-context models and identifies model types that are more robust to positional bias;

- We perform an extensive reproduction study of over 20 ranking models using two established benchmark collections for long-document retrieval and ranking;
- We experiment with an [existing approach](#) to de-biasing training data and motivate further research in this area.

We release our code and data to support further research.²

2 Related Work

Neural Ranking models have been a widely studied topic in recent years (Guo et al., 2019), though the success of early approaches was debated (Lin, 2019). This changed with the introduction of BERT, a bi-directional encoder-only Transformer model (Devlin et al., 2019), which significantly outperformed previous methods in both NLP (Devlin et al., 2019) and information retrieval (IR) tasks (Nogueira et al., 2019; Craswell et al., 2021a).

Several Transformer-based models, such as ELECTRA (Clark et al., 2020) and DEBERTA (He et al., 2021), have improved upon BERT through different training strategies and datasets. However, due to their architectural similarities, we—following Lin et al. (2021)—refer to these collectively as BERT models.

Despite their strong performance, neural models are vulnerable to distribution shifts, often relying on superficial features and exhibiting various *biases*. They do not consistently outperform BM25 on out-of-domain data (Thakur et al., 2021; Mokri et al., 2021), can be misled by minor text modifications and distractor sentences (MacAvaney et al., 2022), or reformulated queries (Penha et al., 2022). They also struggle to effectively utilize information located in the middle of long input contexts (Liu et al., 2024).

A seemingly similar yet distinct issue of positional relevance bias has been identified in information retrieval settings, particularly within the MS MARCO document-retrieval collection (Hofstätter et al., 2020b; Coelho et al., 2024). Some

studies have reported strong performance of *FirstP* baselines on long-document retrieval collections, interpreting this as evidence of benchmark-induced positional bias (Zhu et al., 2024; Rau et al., 2024).

Because positional relevance bias can “obscure” benefits of long-document ranking models, (Rau et al., 2024) proposed to compare these models with *RandP* baselines, which score a randomly selected passage. However, we believe this approach is problematic for two reasons. First, since a *RandP* model often fails to score an entire relevant passage, it artificially underestimates model accuracy, making comparisons with *RandP* unfair. Second, this approach does not address the core problem of biased benchmarks, which still allow models to exploit the shortcut of focusing only on the document’s initial portion.

However, strong performance of *FirstP* baseline is only indirect evidence, potentially resulting from implementation bugs, suboptimal training methods, or model-inherent biases. (Coelho et al., 2024) found that embedding models trained on MS MARCO “dwell” in the beginning and are somewhat less effective when relevant information is present elsewhere in a document. The study used only two embedding models and has additional limitations: (1) it is unclear if the bias is fully attributable to data (2) the models were not tested under conditions of extreme positional bias, (3) no mitigation strategy was evaluated.

To address the issue with existing benchmarks, (Zhu et al., 2024) proposed a *LongEmbed* benchmark with two synthetic tasks where relevant mini-passages were scattered uniformly across documents whose lengths varied from 256 to 32768 tokens. However, as discussed in §B.3 of the Appendix, these synthetic sets are quite unnatural and lack diversity. Furthermore, Zhu et al. (2024) provide only small query sets and no in-domain training data, making it difficult to assess the upper performance bound that models can achieve on this dataset. As another important limitation Zhu et al. (2024), only explored training-free extensions of positional encoding and did not investigate methods to de-bias training data. In contrast, Hofstätter et al. (2021a) proposed to de-bias training data using a simple-yet-effective approach. However, they did *not* evaluate it on *challenging* long-document datasets.

Due to the quadratic complexity of the Transformer’s attention mechanism (Vaswani et al.,

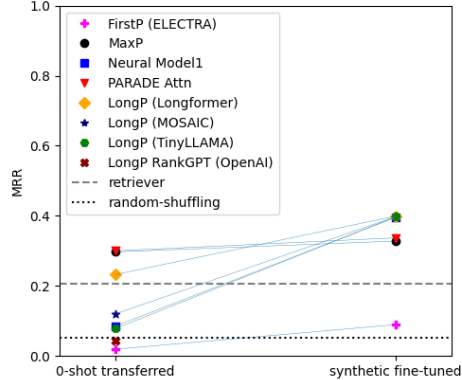
²https://anonymous.4open.science/r/long_doc_rank_model_analysis_v2-78E9/.

237 2017; Bahdanau et al., 2015), early Transformer
 238 models restricted input length to a maximum of
 239 512 (subword) tokens. Until around 2022, two
 240 main strategies were used to process long docu-
 241 ments: (1) localizing attention and (2) splitting
 242 documents into smaller, independently processed
 243 chunks. Attention-localization methods apply a
 244 limited-span (sliding window) attention with se-
 245 lective global attention. Given the vast number of such
 246 approaches (see Tay et al. 2020), evaluating all of
 247 them is impractical. Therefore, we focus on two
 248 popular models: Longformer (Beltagy et al., 2020)
 249 and BigBird (Zaheer et al., 2020). More recently, it
 250 has also become feasible to train long-context mod-
 251 els with (an IO-efficient) FlashAttention algorithm
 252 without sparsifying attention (Dao et al., 2022). In
 253 our work we use two such models: JINA (Günther
 254 et al., 2023) and MOSAIC (Portes et al., 2023).

255 In summary, the methods to tackle longer docu-
 256 ments are divided into *LongP* methods—where
 257 longer document lengths are “natively” supported
 258 and *SplitP* methods—where the longer document
 259 cannot be processed as a whole and needs to be
 260 processed in chunks. The results of each chunk
 261 are aggregated together using various aggregation
 262 techniques, including a computation of a maximum
 263 or a weighted-sum prediction score (Yilmaz et al.,
 264 2019; Dai and Callan, 2019; MacAvaney et al.,
 265 2019). This includes MaxP (Dai and Callan, 2019),
 266 AvgP, SumP (MacAvaney et al., 2019), as well as
 267 PARADE Avg and PARADE Max models (MacA-
 268 vaney et al., 2019). **MaxP is an important baseline**
 269 **that computes relevance scores for each chunk in-**
 270 **dependently and takes their maximum.**

271 Some *SplitP* approaches aggregate using simple
 272 neural networks. This includes all CEDR (MacA-
 273 vaney et al., 2019) models, the Neural Model 1
 274 (Boytsov and Kolter, 2021), and the PARADE At-
 275 tention model (Li et al., 2024). In contrast, PA-
 276 RADE Transformer (Li et al., 2024) models’ aggre-
 277 gator network is an additional Transformer model.
 278 Due to space constraints, a detailed description of
 279 document-splitting (*SplitP*) approaches is provided
 280 in the Appendix § C.

281 The recent success of decoder-only models—
 282 commonly known as LLMs—has led to a new gen-
 283 eration of cross-encoding *LongP* models that na-
 284 tively support longer contexts. First, a pre-trained
 285 cross-encoding decoder-only model can be directly
 286 fine-tuned in a ranking or embedding task (Ma
 287 et al., 2023). Second, the RankGPT approach (Sun



288 Figure 2: Zero-shot vs. fine-tuned performance on MS
 289 MARCO FarRelevant. **This figure shows results for a**
 290 **representative set of models.**

291 **et al., 2023**) formulates document ranking as a
 292 generation task: The model is prompted with a
 293 list of documents and an instruction to generate
 294 their ranking—an ability made possible through
 295 instruction-tuning and/or alignment (Wei et al.,
 296 2022; Ouyang et al., 2022). When the combined
 297 length of concatenated documents exceeds the in-
 298 put context size, RankGPT employs an overlapping
 299 sliding window strategy, followed by aggregation
 300 of the results.

3 Experiments

3.1 Data

301 Our primary datasets, used for both training and
 302 evaluation, consist of several realistic collections
 303 (along with their respective query sets) and syn-
 304 synthetic data. All datasets are in *English*. Document
 305 and query statistics are provided in Appendix § B.1
 306 Tables 9 and 10.

307 The realistic datasets include two versions of the
 308 MS MARCO Documents collection (v1 and v2),
 309 MS MARCO Passages collection (v1), (Bajaj et al.,
 310 2016; Craswell et al., 2020, 2021b), Robust04
 311 (Voorhees, 2004), and the NQ BEIR, which is a
 312 Natural Question (Kwiatkowski et al., 2019) sub-
 313 set incorporated into the BEIR benchmark (Thakur
 314 et al., 2021).

315 Following Hofstätter et al. (2021a), we created
 316 a de-biased version of MS MARCO by randomly
 317 splitting documents at word boundaries and then
 318 concatenating the shuffled segments. This de-
 319 biasing process is only partial, as shorter docu-
 320 ments remain more frequent. To address this imbal-
 321 ance, we experimented with oversampling longer
 322 documents, but this approach did not yield improve-

| Retriever / Ranker | MS MARCO | TREC DL | title | Robust04 | Avg. gain over FirstP |
|---|----------------------------------|----------------------------|----------------------------------|----------------------------------|--------------------------|
| | dev | (2019-2021) | | description | |
| | MRR | NDCG@10 | NDCG@20 | | |
| BM25 retriever (if different from BM25) | 0.274 0.312 | 0.545 0.629 | 0.428 - | 0.402 - | - |
| FirstP (BERT) | 0.394 | 0.632 | 0.475 | 0.527 | - |
| FirstP (Longformer) | 0.404 | 0.643 | 0.483 | 0.540 | - |
| FirstP (ELECTRA) | 0.417 | 0.662 | 0.492 | 0.552 | - |
| FirstP (DEBERTA) | 0.415 | 0.672 | 0.534 | 0.596 | - |
| FirstP (Big-Bird) | 0.408 | 0.656 | 0.507 | 0.560 | - |
| FirstP (JINA) | 0.422 | 0.654 | 0.488 | 0.532 | - |
| FirstP (MOSAIC) | 0.423 | 0.643 | 0.453 | 0.538 | - |
| FirstP (TinyLLAMA) | 0.395 | 0.615 | 0.431 | 0.473 | - |
| FirstP (E5-4K) zero-shot | 0.380 | 0.641 | 0.438 | 0.429 | - |
| FirstP RankGPT (GPT-4o-mini) | - | 0.708 | - | 0.562 | - |
| AvgP | 0.389 (-1.3%) | 0.642 (+1.5%) | 0.478 (+0.5%) | 0.531 (+0.9%) | +0.4% |
| MaxP | 0.392 (-0.4%) | 0.644 ^a (+1.9%) | 0.488 ^a (+2.6%) | 0.544 ^a (+3.3%) | +1.9% |
| MaxP (ELECTRA) | 0.414 (-0.6%) | 0.659 (-0.5%) | 0.502 (+2.0%) | 0.563 (+2.1%) | +0.8% |
| MaxP (DEBERTA) | 0.402 ^a (-3.2%) | 0.671 (-0.1%) | 0.535 (+0.2%) | 0.609 ^a (+2.2%) | -0.2% |
| SumP | 0.390 (-1.0%) | 0.639 (+1.0%) | 0.486 (+2.2%) | 0.538 (+2.1%) | +1.1% |
| CEDR-DRMM | 0.385 ^a (-2.3%) | 0.629 (-0.5%) | 0.466 (-2.0%) | 0.533 (+1.3%) | -0.9% |
| CEDR-KNRM | 0.379 ^a (-3.8%) | 0.630 (-0.3%) | 0.483 (+1.7%) | 0.535 (+1.7%) | -0.2% |
| CEDR-PACRR | 0.395 (+0.3%) | 0.643 ^a (+1.6%) | 0.496 ^a (+4.3%) | 0.549 ^a (+4.2%) | +2.6% |
| Neural Model1 | 0.398 (+0.9%) | 0.650 ^a (+2.8%) | 0.484 (+1.8%) | 0.537 (+1.9%) | +1.8% |
| PARADE Attn | 0.416 ^a (+5.5%) | 0.652 ^a (+3.1%) | 0.503 ^a (+5.7%) | 0.556 ^a (+5.6%) | +5.0% |
| PARADE Attn (ELECTRA) | 0.431 ^a (+3.3%) | 0.680 ^a (+2.7%) | 0.523 ^a (+6.4%) | 0.581 ^a (+5.3%) | +4.4% |
| PARADE Attn (DEBERTA) | 0.422 ^a (+1.6%) | 0.688 ^a (+2.4%) | 0.549^a (+2.9%) | 0.615^a (+3.2%) | +2.5% |
| PARADE Avg | 0.392 (-0.6%) | 0.646 ^a (+2.1%) | 0.483 (+1.5%) | 0.534 (+1.5%) | +1.1% |
| PARADE Max | 0.405 ^a (+2.7%) | 0.655 ^a (+3.5%) | 0.489 ^a (+2.8%) | 0.548 ^a (+4.0%) | +3.3% |
| PARADE Transf-RAND-L2 | 0.419 ^a (+6.3%) | 0.655 ^a (+3.6%) | 0.488 ^a (+2.8%) | 0.548 ^a (+4.1%) | +4.2% |
| PARADE Transf-RAND-L2 (ELECTRA) | 0.433^a (+3.9%) | 0.670 (+1.2%) | 0.523 ^a (+6.3%) | 0.574 ^a (+3.9%) | +3.8% |
| PARADE Transf-PRETR-L6 | 0.402 ^a (+1.9%) | 0.643 (+1.6%) | 0.494 ^a (+4.0%) | 0.554 ^a (+5.1%) | +3.2% |
| LongP (Longformer) | 0.412 ^a (+1.9%) | 0.668 ^a (+3.9%) | 0.500 ^a (+3.6%) | 0.568 ^a (+5.1%) | +3.6% |
| LongP (Big-Bird) | 0.397 ^a (-2.9%) | 0.651 (-0.7%) | 0.452 ^a (-10.9%) | 0.477 ^a (-14.9%) | -7.3% |
| LongP (JINA) | 0.416 ^a (-1.5%) | 0.665 ^a (+1.7%) | 0.503 ^a (+2.9%) | 0.558 ^a (+4.9%) | +2.0% |
| LongP (MOSAIC) | 0.421 (-0.4%) | 0.664 ^a (+3.3%) | 0.456 (+0.6%) | 0.570 ^a (+6.0%) | +2.4% |
| LongP (TinyLLAMA) | 0.402 ^a (+1.7%) | 0.608 (-1.1%) | 0.452 ^a (+4.8%) | 0.505 ^a (+6.7%) | +3.0% |
| LongP (E5-4K) zero-shot | 0.353 ^a (-7.1%) | 0.649 (+1.3%) | 0.439 (+0.1%) | 0.434 (+1.1%) | -1.1% |
| LongP RankGPT (GPT-4o-mini) | - | 0.706 (-0.3%) | - | 0.562 (+0.0%) | -0.1% |

In each column we show a relative gain with respect model’s respective *FirstP* baseline: The last column shows the average relative gain over *FirstP* baselines. Best numbers are in **bold**: Results are averaged over three seeds. Unless specified explicitly, the backbone is **BERT-base**. Statistical significant differences with respect to this baseline are denoted using the superscript **a**. *p*-value threshold is 0.01 for an MS MARCO development collection and 0.05 otherwise.

Table 1: Comparison between long-document models and respective *FirstP* (truncation) baselines. Results for MS MARCO, TREC DL, and Robust04.

ments.

Our synthetic data consists of two subsets from LongEmbed (Zhu et al., 2024) and our newly created MS MARCO FarRelevant collection. All these can be considered a variant of the needle-in-the-haystack tests, where an informational “nugget” is randomly embedded within unrelated text (Saad-Falcon et al., 2024; Zhu et al., 2024; Liu et al., 2024). We use two LongEmbed subsets: Needle and Passkey: Each has 800 question-document pairs with document lengths varying from (approximately) 256 to 32768 tokens.

MS MARCO FarRelevant was created by randomly mixing relevant and non-relevant passages from the MS MARCO *Passage* collection (Craswell et al., 2020) in such a way that (1) each

document contained exactly one relevant passage, (2) this passage did not start before token 512, and (3) the document length was at most 1431 tokens with (see an algorithm in the Appendix § B.2). It has about 0.5 million documents with an average length of 1.1K tokens. Due to MS MARCO datasets having a **non-commercial license**, MS MARCO FarRelevant has the same licensing restriction. In Appendix § B.3, we present dataset examples and argue that—while all these collections share the limitation of not resembling natural documents—MS MARCO FarRelevant offers greater diversity and serves as a more suitable benchmark for evaluating text retrieval systems.

Robust04 is another relatively small dataset containing 0.5 million documents, comprising a mix

| Ranker | MS MARCO dev | | TREC DL (2019-2021) | | FarRelevant zero-shot transf. | | LongEmbed | |
|---|-----------------------------|-----------------------------|------------------------------|--------------|-------------------------------|---------------|-----------|--|
| | MRR | NDCG@10 | MRR | MRR | fine-tuned | Needle | Passkey | |
| BM25 | 0.274 | 0.545 | 0.207 | 0.207 | 0.305 | 0.339 | | |
| Original MS MARCO training set | | | | | | | | |
| FirstP (ELECTRA) | 0.417 | 0.662 | 0.019 | 0.089 | 0.205 | 0.235 | | |
| MaxP (ELECTRA) | 0.414 | 0.659 | 0.328 | 0.349 | 0.331 | 0.338 | | |
| PARADE Attn (ELECTRA) | 0.431 | 0.680 | 0.338 | 0.354 | 0.270 | 0.334 | | |
| PARADE Transf-RAND-L2 (ELECTRA) | 0.433 | 0.670 | 0.229 | 0.432 | 0.321 | 0.333 | | |
| CEDR-KNRM | 0.379 | 0.630 | 0.055 | 0.382 | 0.129 | 0.166 | | |
| De-biased MS MARCO (Hofstätter et al., 2021a) | | | | | | | | |
| MaxP (ELECTRA) | 0.377 ^a (-9.1%) | 0.665 (+0.8%) | 0.321 (-2.1%) | 0.349 | 0.316 (-4.6%) | 0.325 (-3.9%) | | |
| PARADE Attn (ELECTRA) | 0.390 ^a (-9.4%) | 0.653 ^a (-3.9%) | 0.326 (-3.6%) | 0.354 | 0.251 (-7.1%) | 0.330 (-1.0%) | | |
| PARADE Transf-RAND-L2 (ELECTRA) | 0.410 ^a (-5.4%) | 0.677 (+1.0%) | 0.328 ^a (+43.5%) | 0.432 | 0.259 ^a (-19.4%) | 0.331 (-0.7%) | | |
| CEDR-KNRM | 0.269 ^a (-29.0%) | 0.503 ^a (-20.2%) | 0.202 ^a (+268.8%) | 0.382 | 0.121 (-5.8%) | 0.181 (+8.6%) | | |

Except *FirstP* we train each model using the original and the de-biased MS MARCO. For each model trained on the de-biased dataset, we compute a gain (or loss) compared to the same model trained on the original training set. Statistical significance of the differences are denoted using the superscript superscript **a** (*p*-value threshold is 0.05 for TREC DL and 0.01 for other collections). Best numbers are in **bold**: Results are averaged over three seeds.

Table 2: De-biasing effectiveness. Performance of (selected) rankers trained on original and de-biased MS MARCO.

of news articles and government records, some of which are quite lengthy. However, it includes only a limited number of queries (250), making it a challenging benchmark for training models in low-data scenarios. Each query consists of a title and description: the title expresses a concise information need, while the description provides a more detailed request, often written in proper English prose. We use Robust04 in a cross-validation setting with folds created by [Huston and Croft \(2014\)](#) provided via IR-datasets ([MacAvaney et al., 2021](#)).³

MS MARCO v1 was created from the MS MARCO reading comprehension dataset ([Bajaj et al., 2016](#)) and consist of two *related* collections: MS MARCO Passages and MS MARCO Documents. MS MARCO v1 comes with *large* query sets, which is particularly useful for training and testing models in the big-data regime. These query sets consist of question-like queries sampled from the Bing search engine log with subsequent filtering ([Craswell et al., 2021b](#)). Note that queries are not necessarily proper English questions, e.g., “lyme disease symptoms mood”, but they are answerable by a short passage retrieved from a set of about 3.6M Web documents ([Bajaj et al., 2016](#)). MS MARCO v1 test sets were created in two stages, where initially relevance judgments were created for the passage variant of the dataset. Then, document-level relevance labels were created by transferring passage-level relevance to original documents from which passages were extracted.

³In that we do not train Robust04 models from scratch, but rather fine-tune models trained on MS MARCO Documents.

Relevance labels in the training and development sets are “sparse”: There is about one positive example per query without explicit negatives. In addition to sparse relevance judgments—separated into training and developments subsets—there is a small number (98) of queries that have “dense” judgments provided by NIST assessors for TREC 2019 and 2020 deep learning (DL) tracks ([Craswell et al., 2021a](#)).

The MS MARCO v2 collection was created for the TREC 2021 Deep Learning (DL) track ([Craswell et al., 2021b](#)). It is an expanded version of MS MARCO v1 and incorporates a subset of sparse relevance judgments from MS MARCO v1. In the training set, newly added documents lack both positive and negative judgments, introducing a bias where many relevant documents are mistakenly considered non-relevant. As a result, we do not train on v2 data and only use it for testing.

3.2 Setup

We focus cross-encoding rankers, which process queries concatenated with documents ([Nogueira and Cho, 2019](#)). This includes various *SplitP* and *LongP* models discussed in § 2 and in the Appendix § C. As a reference point we also tested a bi-encoder embedding E5-4K model, which had strong performance on LongEmbed benchmark with context sizes under 4K tokens ([Zhu et al., 2024](#)). E5-4K was tested as a ranking model and only in the zero-shot mode (without fine-tuning).

Nearly all rankers are based on BERT models (bi-directional encoder-only Transformer) with 100M–

417 200M parameters (see Table 11). Additionally, we
418 evaluated two types of LLM rankers: (1) a fine-
419 tuned TinyLLAMA model which delivers strong
420 performance relative to its compact size (Zhang
421 et al., 2024) and (2) generative black-box LLMs.
422 For (2), we used OpenAI’s GPT-4o-mini (OpenAI,
423 2023) and Anthropic’s Claude Haiku-3 (Anthropic,
424 2024), both of which support at least a 128K-token
425 input context.

426 We trained each model using *three* seeds, except
427 the bi-encoder model E5 (Zhu et al., 2024) and
428 RankGPT (Sun et al., 2023), which were evaluated
429 only in the zero-shot mode. Due to the high evalua-
430 tion cost (**more than \$1 per one thousand query-
431 document pairs**),⁴ we also did not test RankGPT
432 on some query sets, in particular, excluding MS
433 MARCO dev set, as it is quite large.

434 To compute statistical significance, we averaged
435 query-specific metric values over these seeds. Due
436 to space constraints, additional experimental details
437 are provided in the Appendix § A.1. Moreover, in
438 the main part of the paper we only show results
439 for the mean reciprocal rank (MRR) and the non-
440 discounted cumulative gain at rank k (NDCG@ K).
441 Additional precision-based metrics are presented
442 in the Appendix (see § A.5).

443 3.3 Results

444 **Realistic Datasets.** Our main experimental re-
445 sults for MS MARCO, TREC DL 2019-2021, and
446 Robust04 are presented in Table 1. Fig. 2 and Ta-
447 ble 4 (in the Appendix § A.5) show results for MS
448 MARCO FarRelevant. In the Appendix (see A.3)
449 we also show that we can match or outperform key
450 prior results, which, we believe, boosts the trust-
451 worthiness of our experiments.

452 We abbreviate names of several PARADE mod-
453 els: Note that PARADE ATTN denotes a PARADE
454 Attention model. The PARADE TRANSF or
455 P. TRANSF prefix denotes PARADE Transformer
456 models where an aggregator Transformer can be
457 either trained from scratch (TRANSF-RAND-L2)
458 or initialized with a pretrained model (TRANSF-
459 PRETR-L6). L2 and L6 denote the number of
460 aggregating layers (two and six, respectively).⁵

461 Unless explicitly specified, the backbone Trans-
462 former model for *SplitP* methods is BERT-base
463 (Devlin et al., 2019). Although using other back-
464 bones such as ELECTRA (Clark et al., 2020) and

465 DEBERTA (He et al., 2021) can improve an overall
466 accuracy, we observe a bigger gain compared to a
467 *FirstP* baseline when we use BERT-base (see § A.3
468 in the Appendix).

469 To ease understanding and simplify presentation,
470 we display key results for a representative sample
471 of models in Fig. 3 and Fig. 2 (in § 1). Moreover,
472 in Table 1 we present only a single aggregate num-
473 ber for all TREC DL query sets, which is obtained
474 by combining all the queries and respective relevance
475 judgments (i.e., we post an overall average
476 rather than an average over the mean values for
477 2019, 2020, and 2020). More detailed results, in-
478 cluding both OpenAI and Anthropic RankGPT, are
479 available in Appendix A.5, specifically in Tables 7
480 and 8.

481 From Fig. 3 and Table 1 we learn that the max-
482 imum average gain over respective *FirstP* base-
483 lines is only 5% (when measured using MRR or
484 NDCG@ K). Gains are much smaller for a number
485 of models, which sometimes match or underper-
486 form their *FirstP* baselines on one or more dataset
487 and some of these differences are statistically sig-
488 nificant. In particular, this is true for RankGPT
489 (Sun et al., 2023), CEDR-DRMM, CEDR-KNRM
490 (MacAvaney et al., 2019), JINA (Günther et al.,
491 2023) and MOSAIC (Portes et al., 2023).

492 We can also see that the *LongP* variant of the
493 Longformer model appears to have a relatively
494 strong performance, but so does the *FirstP* ver-
495 sion of Longformer. Thus, we think that a good
496 performance of Longformer on MS MARCO and
497 Robust04 collections can be largely explained by
498 better pretraining compared to the original BERT-
499 base model rather than to its ability to process long
500 contexts. Moreover, FirstP (ELECTRA) and
501 FirstP (DEBERTA) are even more accurate
502 than FirstP (Longformer) and perform comparably
503 well (or better) with chunk-and-aggregate docu-
504 ment models that uses BERT-base as the backbone
505 model. This is a fair comparison aiming to demon-
506 strate that on a typical test collection the benefits of
507 long-context models are so small that comparable
508 benefits can be obtained by finding or training a
509 more effective *FirstP* model. *FirstP* models are
510 more efficient during inference and they can be
511 pretrained using a larger number of tokens for the
512 same cost (so they could perform better).

513 Based on our analysis of positions of first rele-
514 vance passages, we hypothesize that limited ben-
515 efits of long-context models are not due inability

⁴<https://openai.com/api/pricing/>

⁵Note, however, that TRANSF-PRETR-L2 has only four attention heads.

516 to process long context, but rather due to a pos-
517 iational bias of relevant passages, which tended to be
518 among the first 512 document tokens (see Figure 1
519 and Figure 7 in Appendix B.4).

520 **Synthetic Data.** To further support this hypoth-
521 esis, we carried out two sets of experiments us-
522 ing our new MS MARCO FarRelevant collection,
523 where a relevant passage did not start until to-
524 ken 512. We carried out both the zero-shot ex-
525 periment (evaluation of the model trained on MS
526 MARCO) as well fine-tuning experiment using
527 50K in-domain queries (from the MS MARCO
528 FarRelevant).

529 Results for key models are shown in Fig. 2 and
530 more detailed results can be found in Table 4 of
531 the Appendix A.5. The *FirstP* models performed
532 roughly at the random-baseline level in both zero-
533 shot and fine-tuning modes (**RQ1**). Because of
534 this our main baselines here are Longformer and
535 *MaxP* models. For models with ELECTRA and
536 DEBERTA backbones we compare with *MaxP*
537 (ELECTRA) and *MaxP* (DEBERTA), respectively.
538 Otherwise, the baseline is *MaxP* (BERT).

539 Surprisingly, E5-4K performance is also at a
540 random-baseline level despite its competitive per-
541 formance on LongEmbed benchmark (Zhu et al.,
542 2024), MS MARCO, and Robust04 (see Table 1).
543 Both GPT-4o-mini and Claude Haiku-3 RankGPT
544 perform at the random-baseline level as well! As
545 a sanity check, and to verify if more accurate and
546 expensive LLMs could do better, we assessed per-
547 formance of GPT-4o for a sample of 100 queries.
548 The respective RankGPT (Sun et al., 2023) ranker
549 was still not better than a random baseline (**RQ1**).

550 Simple aggregation models including *MaxP*
551 and PARADE Attention had good zero-shot ac-
552 curacy, but benefited little from fine-tuning on MS
553 MARCO FarRelevant (**RQ1**); In contrast, other
554 long-document models had poor zero-shot perfor-
555 mance (sometimes at a random baseline level),
556 but outstripped *respective MaxP* baselines by as
557 much as 13.3%-27.7% after finetuning (**RQ1** and
558 **RQ2**).

559 In contrast, other long-document models had
560 poor zero-shot performance (sometimes at a ran-
561 dom baseline level), but outstripped *respective*
562 *MaxP* baselines by as much as 13.3%-27.7% af-
563 ter finetuning (**RQ1** and **RQ2**)

564 With exception of RankGPT (Sun et al., 2023)
565 on TREC DL 2019-2021, PARADE Transformer
566 models were more effective than other models on

567 standard collections, their advantage was small (a
568 few %). In contrast, on MS MARCO FarRelev-
569 ant, PARADE Transformer (ELECTRA) outper-
570 formed the next competitor Longformer by 8% and
571 PARADE Max (ELECTRA)—an early chunk-and-
572 aggregate approach—by as much as 23.8% (**RQ2**).

573 **Bias Mitigation.** To address **RQ3**, we trained
574 four representative models on a de-biased version
575 of MS MARCO (see Appendix § A.1.3 for selec-
576 tion rationale), using the de-biasing approach by
577 Hofstätter et al. (2021a), and tested them on MS
578 MARCO FarRelevant as well as on Needle/Passkey
579 subsets of LongEmbed (Zhu et al., 2024). We also
580 evaluated four models fine-tuned on MS MARCO
581 FarRelevant on TREC DL 2019-2020 query sets.
582 Due to the substantial NDCG@10 drop (0.1–0.15)
583 observed for PARADE Transformer and CEDR-
584 KNRM, we concluded that fine-tuning on purely
585 synthetic data is not viable and did not pursue it
586 further.

587 According to Table 2, de-biasing improved per-
588 formance of CEDR-KNRM and PARADE Trans-
589 former on MS MARCO FarRelevant. Yet, it mostly
590 caused performance degradation on the original
591 MS MARCO dataset and on LongEmbed subsets.
592 It did not benefit the *MaxP* and PARADE Attention
593 models, which were the most robust to positional
594 bias.

595 We further tested de-biased models on short-
596 document collections using MS MARCO Passage
597 collection and a subset of seven BEIR collections
598 (Thakur et al., 2021). According to Table 3 in Ap-
599 pendix A, for three out of four models de-biasing
600 has either positive or small negative effect (at most
601 1% degradation). In particular, on BEIR NQ sub-
602 set PARADE Transformer and CEDR-KNRM im-
603 proved by 2.5% and 11%, respectively. These
604 results are promising, but they also suggest that
605 mitigating positional bias remains a challenging
606 problem (**RQ3**).

607 **Key Findings.** Based on our results, we make
608 the following key observations:

- 609 • Not only positional bias diminished benefits
610 of supporting longer document contexts, but it
611 also leads to model overfitting to the bias and
612 performing poorly in a zero-shot setting when
613 the distribution of relevant passages changed
614 substantially;
- 615 • In that, we found that de-biasing training data
616 had a mixed success: Although it improved

the effectiveness of some models on some long-document ranking tasks without substantial degradation on short-document collections, it degraded performance in several cases especially for MaxP and PARADE Attention models, which were already intrinsically more robust to relevance position bias.

- It is also worth highlighting the consistently strong performance of PARADE models on both standard long-document collections and MS MARCO FarRelevant. The best PARADE models substantially outperformed the best *LongP* models in both zero-shot and fine-tuning settings, although the specific models leading in each setting may differ.

4 Conclusion

In this work, we revisited the problem of positional relevance bias in long-document retrieval and presented extensive evidence of its *widespread* presence across existing benchmarks. Using both real and synthetic datasets—including our new *diagnostic* dataset, MS MARCO FarRelevant—we evaluated effectiveness of over 20 ranking models as well as their robustness to relevance positional bias.

Our findings highlight the importance of benchmark design that does not obscure the benefits of long-context modeling. We identified model families (i.e., PARADE Attention and MaxP) that are more robust to positional bias, and confirmed the strong performance of PARADE models (Li et al., 2024), which remain competitive even against recent long-context architectures.

Finally, our de-biasing experiments yielded limited and/or inconsistent gains, motivating further research into more effective mitigation strategies, including combining de-biasing with training on well-designed synthetic data.

5 Limitations

Our paper has several limitations related primarily to the choice of datasets, models, and the strength of evidence for the positional bias of relevant passages.

First of all, our evaluation uses only cross-encoding ranking models. With an exception of E5-4K model, which is used in the zero-shot ranking mode, we do not train or evaluate bi-encoding models (typically used to create query and document embeddings for the first-stage retrieval). We

nonetheless believe that—given a large number of proposals for long-document ranking—a reproduction and evaluation of cross-encoding long-document rankers is a sufficiently important topic that alone warrants a publication.

Moreover, as we explain below, we also use cross-encoding rankers as a tool to detect and expose bias in the position of relevant information. In that, cross-encoders are easier to train using standard (rather than high-memory) GPUs with mini-batch size one and gradient accumulation. They also typically require only one epoch to converge (only a few models need two or three epochs). In contrast, bi-encoders are trained using large batches with in-batch negatives for multiple epochs (e.g., Karpukhin et al. (2020) report using at least 40 epochs).

Second, a bulk of our ranking experiments uses only two *English* document collections: MS MARCO Documents v1 and v2 (Craswell et al., 2021b) and Robust04 (Clarke et al., 2004). However, we have to restrict the choice of datasets to make multi-seed evaluations of 20+ models feasible. Yet, to corroborate existence of positional bias we used two additional popular long-document collections: Gov2 (Allan et al., 2008) and ClueWeb12 (Collins-Thompson et al., 2013a). For the study on robustness of model to positional bias and its mitigation, we used two additional synthetic collections: MS MARCO FarRelevant and two subsets from LongEmbed (Zhu et al., 2024) together with short-document collections MS MARCO Passages (v1) (Craswell et al., 2020) and BEIR NQ (Kwiatkowski et al., 2019; Thakur et al., 2021).

One could argue that the limited improvements over *FirstP* baselines result from the models’ inability to handle long contexts. To address this concern, we trained and evaluated a diverse set of cross-encoding ranking models, including both split-and-aggregate models and models explicitly designed for long input sequences. Additionally, we assessed cloud-based RankGPT rankers, which have shown strong performance in recent research (Sun et al., 2023).

However, we can still test only a limited number of models: One might always argue that there are untested architectures that would outperform *FirstP* baselines by a much larger margin. To demonstrate that selected models can, in principle, benefit from long contexts and decisively outperform simple baselines such as *FirstP* and even *MaxP* models we

716
717
718
719
720
721
722
723
724
725
726
727
728
729
730
731
732
733
734
735
736
737
738
739
740
741
742
743
744
745
746
747
748
749
750
751
752
753
754
755
756
757
758
759
760
761
762
763
764
765
766
trained and/or evaluated them on a synthetic collection MS MARCO FarRelevant, which can be seen as a challenging version of a needle-in-the-haystack test. This is still a limiting experiment, because synthetic collections—with documents composed from randomly selected passages—are imperfect proxies for real-life datasets. In Appendix § B.3 we discuss this limitation in detail and, nevertheless, argue that MS MARCO FarRelevant is a more suitable synthetic benchmark for evaluating text retrieval systems compared to LongEmbed subsets Needle and Passkey (Zhu et al., 2024).

In summary, we provided three types of evidence for positional bias of relevant passages: strong performance of *FirstP* models on standard collections, direct estimation of the distribution of relevant passages using substring matching and LLM relevance judges (Upadhyay et al., 2024), as well as experimentation with the synthetic collection MS MARCO FarRelevant where relevant passages distribution was not skewed towards the beginning of a document. Each experiment provided imperfect/limited evidence on its own, but together they strongly supported the existence of relevance position bias.

While our analysis confirms a strong early-position relevance bias across multiple retrieval benchmarks, we acknowledge that this pattern may not generalize to all domains. For example, prior work has shown that in scientific abstracts, both the first and last sentences tend to be crucial (Ruch et al., 2006). Investigating positional relevance patterns in such domains is an important direction for future work.

In our experiments with Robust04 and MS MARCO, we truncated documents to a maximum of 1431 BERT tokens. However, this constraint did not hinder our ability to address key research questions. As detailed in Appendix § A.2, using larger inputs led to only marginal improvements.

Notably, when models trained on MS MARCO were applied to MS MARCO FarRelevant in a zero-shot setting, we observed a significant drop in MRR (at least 17%) across many models. Several models—including RankGPT (Sun et al., 2023)—even failed to outperform a random-shuffling baseline, despite MS MARCO FarRelevant documents containing fewer than 1500 tokens.

Interestingly, despite this token limitation, several long-context models significantly outperformed both *FirstP* and *MaxP* baselines by over

20%. This suggests that even datasets with relatively short documents can serve as a meaningful benchmark for distinguishing strong and weak long-context models—unlike the original MS MARCO, where all models have close accuracy.

6 Ethics Statement

We believe our study does not pose any ethical concerns. We do not collect any new data with the help of human annotators and we do not use human or animal subjects in our study. Although we do discover a positional bias in existing retrieval collections, we are not aware of any potential risks or harms that can be caused by the exposure of this bias.

In terms of the environmental impact, our computational requirements are rather modest, because we only fine-tuned our models rather than trained them from scratch. These models were also rather small by modern standards. Except 1B-parameter TinyLLAMA (Zhang et al., 2024), each model has about 100M parameters (see Table 11 for details). Despite training and testing 20+ models with three seeds, we estimate to have spent only about 6400 GPU hours for our main experiments. 96% of the time we used NVIDIA A10 (or similarly-powerful) RTX 3090 GPUs and 4% of the time we used NVIDIA A6000.

We believe this is roughly equivalent to training a single 1B-parameter TinyLLAMA model, which required about 3400 GPU hours using a more powerful NVIDIA A100. This, in turn, this is only a tiny fraction of compute required to train LLAMA2 models (2% compared to a 7B LLAMA2 smodel).⁶

References

James Allan, Javed A. Aslam, Virgil Pavlu, Evangelos Kanoulas, and Ben Carterette. 2008. Million query track 2008 overview. In *TREC*, volume 500-277 of *NIST Special Publication*. National Institute of Standards and Technology (NIST).

Anthropic. 2024. The claudie 3 model family: Opus, sonnet, haiku.

Negar Arabzadeh and Charles LA Clarke. 2025. Benchmarking llm-based relevance judgment methods. *arXiv preprint arXiv:2504.12558*.

Dzmitry Bahdanau, Kyunghyun Cho, and Yoshua Bengio. 2015. Neural machine translation by jointly

⁶[https://github.com/microsoft/Llama-2-Onnx/
blob/main/MODEL-CARD-META-LLAMA-2.md](https://github.com/microsoft/Llama-2-Onnx/blob/main/MODEL-CARD-META-LLAMA-2.md)

| | | |
|-----|---|-----|
| 814 | learning to align and translate. In <i>3rd International Conference on Learning Representations, ICLR 2015</i> . | 870 |
| 815 | | 871 |
| 816 | | 872 |
| 817 | Payal Bajaj, Daniel Campos, Nick Craswell, Li Deng, Jianfeng Gao, Xiaodong Liu, Rangan Majumder, Andrew McNamara, Bhaskar Mitra, Tri Nguyen, et al. 2016. MS MARCO: A human generated machine reading comprehension dataset. <i>arXiv preprint arXiv:1611.09268</i> . | 873 |
| 818 | | 874 |
| 819 | | 875 |
| 820 | | |
| 821 | | |
| 822 | | |
| 823 | Iz Beltagy, Matthew E. Peters, and Arman Cohan. 2020. Longformer: The long-document transformer. <i>CoRR</i> , abs/2004.05150. | 876 |
| 824 | | 877 |
| 825 | | 878 |
| 826 | Adam Berger and John Lafferty. 1999. Information retrieval as statistical translation. In <i>Proceedings of the 22nd annual international ACM SIGIR conference on Research and development in information retrieval</i> , pages 222–229. | 879 |
| 827 | | 880 |
| 828 | | 881 |
| 829 | | 882 |
| 830 | | 883 |
| 831 | Leonid Boytsov and Zico Kolter. 2021. Exploring classic and neural lexical translation models for information retrieval: Interpretability, effectiveness, and efficiency benefits. In <i>ECIR (1)</i> , volume 12656 of <i>Lecture Notes in Computer Science</i> , pages 63–78. Springer. | 884 |
| 832 | | 885 |
| 833 | | 886 |
| 834 | | 887 |
| 835 | | |
| 836 | | |
| 837 | Peter F. Brown, Stephen Della Pietra, Vincent J. Della Pietra, and Robert L. Mercer. 1993. The mathematics of statistical machine translation: Parameter estimation. <i>Computational Linguistics</i> , 19(2):263–311. | 888 |
| 838 | | 889 |
| 839 | | 890 |
| 840 | | 891 |
| 841 | Kevin Clark, Minh-Thang Luong, Quoc V. Le, and Christopher D. Manning. 2020. ELECTRA: pre-training text encoders as discriminators rather than generators. In <i>ICLR</i> . OpenReview.net. | 892 |
| 842 | | 893 |
| 843 | | 894 |
| 844 | | |
| 845 | Charles L. A. Clarke, Nick Craswell, and Ian Soboroff. 2004. Overview of the TREC 2004 terabyte track. In <i>TREC</i> , volume 500-261 of <i>NIST Special Publication</i> . National Institute of Standards and Technology (NIST). | 895 |
| 846 | | 896 |
| 847 | | 897 |
| 848 | | |
| 849 | | |
| 850 | João Coelho, Bruno Martins, João Magalhães, Jamie Callan, and Chenyan Xiong. 2024. Dwell in the beginning: How language models embed long documents for dense retrieval. In <i>ACL (Short Papers)</i> , pages 370–377. Association for Computational Linguistics. | 902 |
| 851 | | 903 |
| 852 | | 904 |
| 853 | | 905 |
| 854 | | |
| 855 | | |
| 856 | Kevyn Collins-Thompson, Paul N. Bennett, Fernando Diaz, Charlie Clarke, and Ellen M. Voorhees. 2013a. TREC 2013 web track overview. In <i>TREC</i> , volume 500-302 of <i>NIST Special Publication</i> . National Institute of Standards and Technology (NIST). | 910 |
| 857 | | 911 |
| 858 | | 912 |
| 859 | | 913 |
| 860 | | 914 |
| 861 | Kevyn Collins-Thompson, Paul N. Bennett, Fernando Diaz, Charlie Clarke, and Ellen M. Voorhees. 2013b. TREC 2013 web track overview. In <i>TREC</i> , volume 500-302 of <i>NIST Special Publication</i> . National Institute of Standards and Technology (NIST). | 915 |
| 862 | | 916 |
| 863 | | 917 |
| 864 | | |
| 865 | | |
| 866 | Ronan Collobert, Jason Weston, Léon Bottou, Michael Karlen, Koray Kavukcuoglu, and Pavel Kuksa. 2011. Natural language processing (almost) from scratch. <i>J. Mach. Learn. Res.</i> , 12:2493–2537. | 918 |
| 867 | | 919 |
| 868 | | 920 |
| 869 | | 921 |
| | | 922 |
| | | 923 |
| | | |
| | Nick Craswell, Bhaskar Mitra, Emine Yilmaz, and Daniel Campos. 2021a. Overview of the TREC 2020 deep learning track. <i>CoRR</i> , abs/2102.07662. | |
| | | |
| | Nick Craswell, Bhaskar Mitra, Emine Yilmaz, Daniel Campos, and Jimmy Lin. 2021b. Overview of the TREC 2021 deep learning track. | |
| | | |
| | Nick Craswell, Bhaskar Mitra, Emine Yilmaz, Daniel Campos, Jimmy Lin, Ellen M. Voorhees, and Ian Soboroff. 2022. <i>Overview of the TREC 2022 deep learning track</i> . In <i>Proceedings of the Thirty-First Text REtrieval Conference, TREC 2022, online, November 15-19, 2022</i> , volume 500-338 of <i>NIST Special Publication</i> . National Institute of Standards and Technology (NIST). | |
| | | |
| | Nick Craswell, Bhaskar Mitra, Emine Yilmaz, Daniel Campos, and Ellen M. Voorhees. 2020. Overview of the TREC 2019 deep learning track. <i>CoRR</i> , abs/2003.07820. | |
| | | |
| | Nick Craswell, Bhaskar Mitra, Emine Yilmaz, Hossein A. Rahmani, Daniel Campos, Jimmy Lin, Ellen M. Voorhees, and Ian Soboroff. 2023. Overview of the TREC 2023 deep learning track. In <i>TREC</i> , volume 500-xxx of <i>NIST Special Publication</i> . National Institute of Standards and Technology (NIST). | |
| | | |
| | Zhuyun Dai and Jamie Callan. 2019. Deeper text understanding for IR with contextual neural language modeling. In <i>SIGIR</i> , pages 985–988. ACM. | |
| | | |
| | Tri Dao, Daniel Y. Fu, Stefano Ermon, Atri Rudra, and Christopher Ré. 2022. Flashattention: Fast and memory-efficient exact attention with io-awareness. In <i>NeurIPS</i> . | |
| | | |
| | Jacob Devlin, Ming-Wei Chang, Kenton Lee, and Kristina Toutanova. 2019. BERT: pre-training of deep bidirectional transformers for language understanding. pages 4171–4186. | |
| | | |
| | Thibault Formal, Carlos Lassance, Benjamin Piwowarski, and Stéphane Clinchant. 2021. SPLADE v2: Sparse lexical and expansion model for information retrieval. <i>CoRR</i> , abs/2109.10086. | |
| | | |
| | Chengzhen Fu, Enrui Hu, Letian Feng, Zhicheng Dou, Yantao Jia, Lei Chen, Fan Yu, and Zhao Cao. 2022. Leveraging multi-view inter-passage interactions for neural document ranking. In <i>Proceedings of the Fifteenth ACM International Conference on Web Search and Data Mining, WSDM '22</i> , page 298–306, New York, NY, USA. Association for Computing Machinery. | |
| | | |
| | Luyu Gao and Jamie Callan. 2022. Long document re-ranking with modular re-ranker. In <i>Proceedings of the 45th International ACM SIGIR Conference on Research and Development in Information Retrieval, SIGIR '22</i> , page 2371–2376, New York, NY, USA. Association for Computing Machinery. | |
| | | |

| | | |
|------|--|------|
| 924 | Jiafeng Guo, Yixing Fan, Qingyao Ai, and W. Bruce Croft. 2016. A deep relevance matching model for ad-hoc retrieval. In <i>CIKM</i> , pages 55–64. ACM. | 980 |
| 925 | | 981 |
| 926 | | 982 |
| 927 | Jiafeng Guo, Yixing Fan, Liang Pang, Liu Yang, Qingyao Ai, Hamed Zamani, Chen Wu, W Bruce Croft, and Xueqi Cheng. 2019. A deep look into neural ranking models for information retrieval. <i>Information Processing & Management</i> , page 102067. | 983 |
| 928 | | 984 |
| 929 | | 985 |
| 930 | | |
| 931 | | |
| 932 | Mandy Guo, Joshua Ainslie, David Uthus, Santiago Ontanon, Jianmo Ni, Yun-Hsuan Sung, and Yinfei Yang. 2022. <i>LongT5: Efficient text-to-text transformer for long sequences</i> . In <i>Findings of the Association for Computational Linguistics: NAACL 2022</i> , pages 724–736, Seattle, United States. Association for Computational Linguistics. | 986 |
| 933 | | 987 |
| 934 | | 988 |
| 935 | | |
| 936 | | |
| 937 | | |
| 938 | | |
| 939 | Michael Günther, Jackmin Ong, Isabelle Mohr, Alaeddine Abdessalem, Tanguy Abel, Mohammad Kalim Akram, Susana Guzman, Georgios Mastrapas, Saba Sturua, Bo Wang, Maximilian Werk, Nan Wang, and Han Xiao. 2023. <i>Jina embeddings 2: 8192-token general-purpose text embeddings for long documents</i> . | 989 |
| 940 | | 990 |
| 941 | | 991 |
| 942 | | 992 |
| 943 | | 993 |
| 944 | | 994 |
| 945 | | |
| 946 | Pengcheng He, Jianfeng Gao, and Weizhu Chen. 2021. <i>Debertav3: Improving deberta using electra-style pre-training with gradient-disentangled embedding sharing</i> . | 995 |
| 947 | | 996 |
| 948 | | 997 |
| 949 | | 998 |
| 950 | Sebastian Hofstätter, Aldo Lipani, Sophia Althammer, Markus Zlabinger, and Allan Hanbury. 2021a. Mitigating the position bias of transformer models in passage re-ranking. In <i>ECIR (1)</i> , volume 12656 of <i>Lecture Notes in Computer Science</i> , pages 238–253. Springer. | 999 |
| 951 | | 1000 |
| 952 | | 1001 |
| 953 | | 1002 |
| 954 | | 1003 |
| 955 | | 1004 |
| 956 | Sebastian Hofstätter, Bhaskar Mitra, Hamed Zamani, Nick Craswell, and Allan Hanbury. 2021b. Intra-document cascading: Learning to select passages for neural document ranking. In <i>SIGIR</i> , pages 1349–1358. ACM. | 1005 |
| 957 | | 1006 |
| 958 | | 1007 |
| 959 | | |
| 960 | | |
| 961 | Sebastian Hofstätter, Markus Zlabinger, and Allan Hanbury. 2020a. Interpretable & time-budget-constrained contextualization for re-ranking. In <i>ECAI</i> , volume 325 of <i>Frontiers in Artificial Intelligence and Applications</i> , pages 513–520. IOS Press. | 1012 |
| 962 | | 1013 |
| 963 | | 1014 |
| 964 | | |
| 965 | | |
| 966 | Sebastian Hofstätter, Markus Zlabinger, Mete Sertkan, Michael Schröder, and Allan Hanbury. 2020b. Fine-grained relevance annotations for multi-task document ranking and question answering. In <i>CIKM</i> , pages 3031–3038. ACM. | 1015 |
| 967 | | 1016 |
| 968 | | 1017 |
| 969 | | 1018 |
| 970 | | |
| 971 | Kai Hui, Andrew Yates, Klaus Berberich, and Gerard de Melo. 2018. Co-pacrr: A context-aware neural IR model for ad-hoc retrieval. In <i>WSDM</i> , pages 279–287. ACM. | 1019 |
| 972 | | 1020 |
| 973 | | 1021 |
| 974 | | 1022 |
| 975 | Samuel Huston and W Bruce Croft. 2014. A comparison of retrieval models using term dependencies. In <i>Proceedings of the 23rd ACM International Conference on Conference on Information and Knowledge Management</i> , pages 111–120. | 1023 |
| 976 | | |
| 977 | | |
| 978 | | |
| 979 | | |
| 980 | Nasreen Abdul Jaleel, James Allan, W. Bruce Croft, Fernando Diaz, Leah S. Larkey, Xiaoyan Li, Mark D. Smucker, and Courtney Wade. 2004. Umass at TREC 2004: Novelty and HARD. In <i>TREC</i> , volume 500–261 of <i>NIST Special Publication</i> . National Institute of Standards and Technology (NIST). | 981 |
| 981 | | 982 |
| 982 | | 983 |
| 983 | | 984 |
| 984 | | 985 |
| 985 | | |
| 986 | Kalervo Järvelin and Jaana Kekäläinen. 2002. Cumulated gain-based evaluation of IR techniques. <i>ACM Trans. Inf. Syst.</i> , 20(4):422–446. | 986 |
| 987 | | 987 |
| 988 | | 988 |
| 989 | Vladimir Karpukhin, Barlas Oguz, Sewon Min, Patrick S. H. Lewis, Ledell Wu, Sergey Edunov, Danqi Chen, and Wen-tau Yih. 2020. Dense passage retrieval for open-domain question answering. In <i>EMNLP (1)</i> , pages 6769–6781. Association for Computational Linguistics. | 989 |
| 990 | | 990 |
| 991 | | 991 |
| 992 | | 992 |
| 993 | | 993 |
| 994 | | 994 |
| 995 | Omar Khattab and Matei Zaharia. 2020. Colbert: Efficient and effective passage search via contextualized late interaction over BERT. In <i>SIGIR</i> , pages 39–48. ACM. | 995 |
| 996 | | 996 |
| 997 | | 997 |
| 998 | | 998 |
| 999 | Tom Kwiatkowski, Jennimaria Palomaki, Olivia Redfield, Michael Collins, Ankur P. Parikh, Chris Alberti, Danielle Epstein, Illia Polosukhin, Jacob Devlin, Kenton Lee, Kristina Toutanova, Llion Jones, Matthew Kelcey, Ming-Wei Chang, Andrew M. Dai, Jakob Uszkoreit, Quoc Le, and Slav Petrov. 2019. <i>Natural questions: a benchmark for question answering research</i> . <i>Trans. Assoc. Comput. Linguistics</i> , 7:452–466. | 999 |
| 1000 | | 1000 |
| 1001 | | 1001 |
| 1002 | | 1002 |
| 1003 | | 1003 |
| 1004 | | 1004 |
| 1005 | | 1005 |
| 1006 | | 1006 |
| 1007 | | 1007 |
| 1008 | Canjia Li, Andrew Yates, Sean MacAvaney, Ben He, and Yingfei Sun. 2024. <i>PARADE: passage representation aggregation for document reranking</i> . <i>ACM Trans. Inf. Syst.</i> , 42(2):36:1–36:26. | 1008 |
| 1009 | | 1009 |
| 1010 | | 1010 |
| 1011 | | 1011 |
| 1012 | Jimmy Lin. 2019. The neural hype and comparisons against weak baselines. In <i>ACM SIGIR Forum</i> , volume 52, pages 40–51. ACM New York, NY, USA. | 1012 |
| 1013 | | 1013 |
| 1014 | | 1014 |
| 1015 | Jimmy Lin, Rodrigo Nogueira, and Andrew Yates. 2021. <i>Pretrained Transformers for Text Ranking: BERT and Beyond</i> . Synthesis Lectures on Human Language Technologies. Morgan & Claypool Publishers. | 1015 |
| 1016 | | 1016 |
| 1017 | | 1017 |
| 1018 | | 1018 |
| 1019 | Nelson F. Liu, Kevin Lin, John Hewitt, Ashwin Paranjape, Michele Bevilacqua, Fabio Petroni, and Percy Liang. 2024. Lost in the middle: How language models use long contexts. <i>Trans. Assoc. Comput. Linguistics</i> , 12:157–173. | 1019 |
| 1020 | | 1020 |
| 1021 | | 1021 |
| 1022 | | 1022 |
| 1023 | | 1023 |
| 1024 | Yinhan Liu, Myle Ott, Naman Goyal, Jingfei Du, Mandar Joshi, Danqi Chen, Omer Levy, Mike Lewis, Luke Zettlemoyer, and Veselin Stoyanov. 2019. Roberta: A robustly optimized BERT pretraining approach. <i>CoRR</i> , abs/1907.11692. | 1024 |
| 1025 | | 1025 |
| 1026 | | 1026 |
| 1027 | | 1027 |
| 1028 | | 1028 |
| 1029 | Ilya Loshchilov and Frank Hutter. 2017. Decoupled weight decay regularization. <i>arXiv preprint arXiv:1711.05101</i> . | 1029 |
| 1030 | | 1030 |
| 1031 | | 1031 |
| 1032 | Xueguang Ma, Liang Wang, Nan Yang, Furu Wei, and Jimmy Lin. 2023. Fine-tuning llama for multi-stage text retrieval. <i>CoRR</i> , abs/2310.08319. | 1032 |
| 1033 | | 1033 |
| 1034 | | 1034 |

| | | |
|------|---|------|
| 1035 | Sean MacAvaney, Sergey Feldman, Nazli Goharian, Doug Downey, and Arman Cohan. 2022. ABNIRML: analyzing the behavior of neural IR models. <i>Trans. Assoc. Comput. Linguistics</i> , 10:224–239. | 1090 |
| 1036 | | 1091 |
| 1037 | | 1092 |
| 1038 | | 1093 |
| 1039 | | 1094 |
| 1040 | Sean MacAvaney, Andrew Yates, Arman Cohan, and Nazli Goharian. 2019. CEDR: contextualized embeddings for document ranking. In <i>SIGIR</i> , pages 1101–1104. ACM. | 1095 |
| 1041 | | 1096 |
| 1042 | | 1097 |
| 1043 | | 1098 |
| 1044 | Sean MacAvaney, Andrew Yates, Sergey Feldman, Doug Downey, Arman Cohan, and Nazli Goharian. 2021. Simplified data wrangling with ir-datasets. In <i>SIGIR</i> . | 1099 |
| 1045 | | 1100 |
| 1046 | | |
| 1047 | Tomas Mikolov, Ilya Sutskever, Kai Chen, Gregory S. Corrado, and Jeffrey Dean. 2013. Distributed representations of words and phrases and their compositionality. In <i>NIPS</i> , pages 3111–3119. | 1101 |
| 1048 | | 1102 |
| 1049 | | 1103 |
| 1050 | | 1104 |
| 1051 | Iurii Mokrii, Leonid Boytsov, and Pavel Braslavski. 2021. <i>A Systematic Evaluation of Transfer Learning and Pseudo-Labeling with BERT-Based Ranking Models</i> , page 2081–2085. Association for Computing Machinery, New York, NY, USA. | 1105 |
| 1052 | | 1106 |
| 1053 | | 1107 |
| 1054 | | 1108 |
| 1055 | | 1109 |
| 1056 | Marius Mosbach, Maksym Andriushchenko, and Dietrich Klakow. 2020. On the stability of fine-tuning BERT: misconceptions, explanations, and strong baselines. <i>CoRR</i> , abs/2006.04884. | 1110 |
| 1057 | | 1111 |
| 1058 | | |
| 1059 | | |
| 1060 | Rodrigo Nogueira and Kyunghyun Cho. 2019. Passage re-ranking with BERT. <i>CoRR</i> , abs/1901.04085. | 1112 |
| 1061 | | 1113 |
| 1062 | | 1114 |
| 1063 | | 1115 |
| 1064 | | |
| 1065 | Rodrigo Nogueira and Jimmy Lin. 2019. From doc2query to docTTTTquery. <i>MS MARCO passage retrieval task publication</i> . | 1116 |
| 1066 | | 1117 |
| 1067 | | 1118 |
| 1068 | Rodrigo Nogueira, Wei Yang, Jimmy Lin, and Kyunghyun Cho. 2019. Document expansion by query prediction. <i>CoRR</i> , abs/1904.08375. | 1119 |
| 1069 | | 1120 |
| 1070 | | 1121 |
| 1071 | | 1122 |
| 1072 | | 1123 |
| 1073 | OpenAI. 2023. <i>GPT-4 technical report</i> . <i>CoRR</i> , abs/2303.08774. | 1124 |
| 1074 | | 1125 |
| 1075 | | 1126 |
| 1076 | | |
| 1077 | Long Ouyang, Jeffrey Wu, Xu Jiang, Diogo Almeida, Carroll L. Wainwright, Pamela Mishkin, Chong Zhang, Sandhini Agarwal, Katarina Slama, Alex Ray, John Schulman, Jacob Hilton, Fraser Kelton, Luke Miller, Maddie Simens, Amanda Askell, Peter Welinder, Paul F. Christiano, Jan Leike, and Ryan Lowe. 2022. Training language models to follow instructions with human feedback. In <i>NeurIPS</i> . | 1127 |
| 1078 | | 1128 |
| 1079 | | 1129 |
| 1080 | | 1130 |
| 1081 | | |
| 1082 | Adam Paszke, Sam Gross, Francisco Massa, Adam Lerer, James Bradbury, Gregory Chanan, Trevor Killeen, Zeming Lin, Natalia Gimelshein, Luca Antiga, et al. 2019. Pytorch: An imperative style, high-performance deep learning library. In <i>Advances in neural information processing systems</i> , pages 8026–8037. | 1131 |
| 1083 | | 1132 |
| 1084 | | 1133 |
| 1085 | Jianlin Su, Murtadha H. M. Ahmed, Yu Lu, Shengfeng Pan, Wen Bo, and Yunfeng Liu. 2024. Roformer: Enhanced transformer with rotary position embedding. <i>Neurocomputing</i> , 568:127063. | 1134 |
| 1086 | | 1135 |
| 1087 | | 1136 |
| 1088 | | 1137 |
| 1089 | Jianlin Su, Yu Lu, Shengfeng Pan, Ahmed Murtadha, Bo Wen, and Yunfeng Liu. 2023. Roformer: Enhanced transformer with rotary position embedding. | 1138 |
| 1090 | Weiwei Sun, Lingyong Yan, Xinyu Ma, Shuaiqiang Wang, Pengjie Ren, Zhumin Chen, Dawei Yin, and Zhaochun Ren. 2023. Is chatgpt good at search? investigating large language models as re-ranking agents. In <i>EMNLP</i> , pages 14918–14937. Association for Computational Linguistics. | 1139 |
| 1091 | | 1140 |
| 1092 | | 1141 |
| 1093 | | 1142 |
| 1094 | | 1143 |

| | | |
|------|--|------|
| 1144 | Yi Tay, Mostafa Dehghani, Dara Bahri, and Donald Metzler. 2020. Efficient transformers: A survey. <i>CoRR</i> , abs/2009.06732. | 1200 |
| 1145 | | 1201 |
| 1146 | | 1202 |
| 1147 | Nandan Thakur, Nils Reimers, Andreas Rücklé, Abhishek Srivastava, and Iryna Gurevych. 2021. BEIR: A heterogeneous benchmark for zero-shot evaluation of information retrieval models. In <i>NeurIPS Datasets and Benchmarks</i> . | 1203 |
| 1148 | | 1204 |
| 1149 | | |
| 1150 | | |
| 1151 | | |
| 1152 | Shivani Upadhyay, Ronak Pradeep, Nandan Thakur, Nick Craswell, and Jimmy Lin. 2024. UMBRELA: umbrela is the (open-source reproduction of the) bing relevance assessor. <i>CoRR</i> , abs/2406.06519. | 1205 |
| 1153 | | 1206 |
| 1154 | | 1207 |
| 1155 | | 1208 |
| 1156 | Ashish Vaswani, Noam Shazeer, Niki Parmar, Jakob Uszkoreit, Llion Jones, Aidan N Gomez, Łukasz Kaiser, and Illia Polosukhin. 2017. Attention is all you need. In <i>NIPS</i> , pages 5998–6008. | 1209 |
| 1157 | | |
| 1158 | | |
| 1159 | | |
| 1160 | Ellen Voorhees. 2004. Overview of the trec 2004 robust retrieval track. In <i>TREC</i> . | 1210 |
| 1161 | | 1211 |
| 1162 | Jason Wei, Maarten Bosma, Vincent Y. Zhao, Kelvin Guu, Adams Wei Yu, Brian Lester, Nan Du, Andrew M. Dai, and Quoc V. Le. 2022. Finetuned language models are zero-shot learners. In <i>ICLR</i> . OpenReview.net. | 1212 |
| 1163 | | 1213 |
| 1164 | | 1214 |
| 1165 | | |
| 1166 | | |
| 1167 | Thomas Wolf, Lysandre Debut, Victor Sanh, Julien Chaumond, Clement Delangue, Anthony Moi, Pierrette Cistac, Tim Rault, Rémi Louf, Morgan Funtowicz, Joe Davison, Sam Shleifer, Patrick von Platen, Clara Ma, Yacine Jernite, Julien Plu, Canwen Xu, Teven Le Scao, Sylvain Gugger, Mariama Drame, Quentin Lhoest, and Alexander M. Rush. 2019. Huggingface’s transformers: State-of-the-art natural language processing. <i>ArXiv</i> , abs/1910.03771. | 1215 |
| 1168 | | 1216 |
| 1169 | | 1217 |
| 1170 | | |
| 1171 | | |
| 1172 | | |
| 1173 | | |
| 1174 | | |
| 1175 | | |
| 1176 | Yonghui Wu, Mike Schuster, Zhifeng Chen, Quoc V. Le, Mohammad Norouzi, Wolfgang Macherey, Maxim Krikun, Yuan Cao, Qin Gao, Klaus Macherey, Jeff Klingner, Apurva Shah, Melvin Johnson, Xiaobing Liu, Lukasz Kaiser, Stephan Gouws, Yoshiaki Kato, Taku Kudo, Hideto Kazawa, Keith Stevens, George Kurian, Nishant Patil, Wei Wang, Cliff Young, Jason Smith, Jason Riesa, Alex Rudnick, Oriol Vinyals, Greg Corrado, Macduff Hughes, and Jeffrey Dean. 2016. Google’s neural machine translation system: Bridging the gap between human and machine translation. <i>CoRR</i> , abs/1609.08144. | 1223 |
| 1177 | | 1224 |
| 1178 | | 1225 |
| 1179 | | 1226 |
| 1180 | | |
| 1181 | | |
| 1182 | | |
| 1183 | | |
| 1184 | | |
| 1185 | | |
| 1186 | | |
| 1187 | | |
| 1188 | Chenyan Xiong, Zhuyun Dai, Jamie Callan, Zhiyuan Liu, and Russell Power. 2017. End-to-end neural ad-hoc ranking with kernel pooling. In <i>SIGIR</i> , pages 55–64. ACM. | 1227 |
| 1189 | | 1228 |
| 1190 | | 1229 |
| 1191 | | 1230 |
| 1192 | Lee Xiong, Chenyan Xiong, Ye Li, Kwok-Fung Tang, Jialin Liu, Paul N. Bennett, Junaid Ahmed, and Arnold Overwijk. 2021. Approximate nearest neighbor negative contrastive learning for dense text retrieval. In <i>ICLR</i> . OpenReview.net. | 1231 |
| 1193 | | |
| 1194 | | |
| 1195 | | |
| 1196 | | |
| 1197 | Zhichao Xu. 2024. Rankmamba: Benchmarking mamba’s document ranking performance in the era of transformers. <i>arXiv preprint arXiv:2403.18276</i> . | 1232 |
| 1198 | | 1233 |
| 1199 | | |
| | A Experiments: Additional Information, Ablations, and Detailed Results | 1234 |
| | A.1 Detailed Training and Evaluation Setup | 1235 |
| | A.1.1 General Setup | 1236 |
| | In our work, a ranker is applied to the output of the first-stage retrieval model, also known as a candidate-generator. Depending on the experiment and the dataset we use different candidate generators: for MS MARCO v1 and Robust04 we used a BM25 ranker (Robertson, 2004). In that, for MS MARCO v1 it was applied to documents expanded using the doc2query approach (Nogueira and Lin, 2019). For MS MARCO v2, we used a hybrid retriever where candidate records are first produced using a k-NN search and subsequently re-ranked using a linear fusion of BM25 scores and the cosine similarity between query and document embeddings. Embeddings were generated using ANCE (Xiong et al., 2021). | 1237 |
| | | 1238 |
| | | 1239 |
| | | 1240 |
| | | 1241 |
| | | 1242 |
| | | 1243 |
| | | 1244 |
| | | 1245 |
| | | 1246 |
| | | 1247 |
| | | 1248 |
| | | 1249 |
| | | 1250 |

| Ranker | TREC DL (2019-2020) | NQ | BEIR (without NQ) | | | | | | | average |
|---|----------------------------|-----------------------------|-------------------|--------------------------|--------------------|--------------------|--------------------|--------------------|---------------|---------|
| | NDCG@10 | NDCG@10 | Touche | COVID | NFC | DBP | SciFact | SciDocs | | |
| BM25 | 0.519 | 0.325 | 0.336 | 0.677 | 0.326 | 0.339 | 0.655 | 0.160 | 0.417 | |
| Original MS MARCO training set | | | | | | | | | | |
| MaxP (ELECTRA) | 0.715 | 0.514 | 0.314 | 0.744 | 0.312 | 0.404 | 0.659 | 0.153 | 0.477 | |
| PARADE Attn (ELECTRA) | 0.710 | 0.496 | 0.356 | 0.743 | 0.266 | 0.386 | 0.606 | 0.140 | 0.463 | |
| PARADE Transf-RAND-L2 (ELECTRA) | 0.703 | 0.474 | 0.293 | 0.728 | 0.297 | 0.380 | 0.658 | 0.154 | 0.461 | |
| CEDR-KNRM | 0.599 | 0.318 | 0.242 | 0.710 | 0.268 | 0.305 | 0.478 | 0.127 | 0.381 | |
| De-biased MS MARCO (Hofstätter et al., 2021a) | | | | | | | | | | |
| MaxP (ELECTRA) | 0.716 (+0.1%) | 0.516 (+0.6%) | 0.309 | 0.742 | 0.296 ^a | 0.408 | 0.646 | 0.150 | 0.473 (-0.8%) | |
| PARADE Attn (ELECTRA) | 0.675 ^a (-4.9%) | 0.427 ^a (-14.0%) | 0.335 | 0.742 | 0.226 ^a | 0.353 ^a | 0.522 ^a | 0.122 ^a | 0.425 (-8.2%) | |
| PARADE Transf-RAND-L2 (ELECTRA) | 0.706 (+0.4%) | 0.485 ^a (+2.5%) | 0.299 | 0.753^a | 0.288 ^a | 0.393 ^a | 0.643 | 0.153 | 0.465 (+0.9%) | |
| CEDR-KNRM | 0.604 (+0.7%) | 0.353 ^a (+11.0%) | 0.231 | 0.683 ^a | 0.265 | 0.340 ^a | 0.419 ^a | 0.122 ^a | 0.377 (-1.0%) | |

We train each model using the original and the de-biased MS MARCO. For each model trained on the de-biased dataset, we compute a gain (or loss) compared to the same model trained on the original training set. Statistical significance of the differences are denoted using the superscript superscript **a** (except TREC DL and TREC COVID that have p -value threshold of 0.05, the p -value threshold is 0.01). Best numbers are in **bold**: Results are averaged over three seeds.

Table 3: De-biasing impact on short-document collection performance. The table shows effectiveness of (selected) rankers trained on original and de-biased MS MARCO (and tested on short-document collections).

Depending on the collection we computed a subset of the following metrics: the mean reciprocal rank (MRR), the non-discounted cumulative gain at rank k (NDCG@K) (Järvelin and Kekäläinen, 2002), the mean average precision (MAP), and precision at rank ($P@K$), $k \in \{10, 20\}$. Due to space constraints, we included results with MAP and $P@K$ only in the Appendix (see § A.5). Note that for test sets with sparse labels (MS MARCO development set and MS MARCO FarRelevant) we computed only MRR.

All experiments were carried out using the an **anonymous** retrieval toolkit framework, which employed Lucene and an **anonymous** toolkit for k-NN search to provide retrieval capabilities. Deep learning support was provided via PyTorch (Paszke et al., 2019) and HuggingFace Transformers library (Wolf et al., 2019). The instructions to reproduce our key results are publicly available in the on-line appendix.⁷

A.1.2 Model Training

A ranker was trained to distinguish between positive examples (known relevant documents) and hard negative examples (documents not marked as relevant) sampled from the set of top- k candidates returned by the candidate generator. We used $k = 100$ for MS MARCO and MS MARCO Far-Relevant and $k = 1000$ for Robust04 (based on preliminary experiments).

Each model was trained using *three* seeds. All

models except MOSAIC were trained using half-precision. MOSAIC models were trained using full-precision. MOSAIC training was unstable (even though we used the full precision) and often resulted in close-to-zero performance. For this reason we continued training with *more* seeds until we obtained three models with reasonable performance. This seed selection strategy could potentially have biased (up) MOSAIC results. To compute statistical significance, we averaged query-specific metric values over these seeds.

All MS MARCO models were trained from scratch. Then these models were fine-tuned on Robust04. Note that except for the aggregation Transformers and TinyLLAMA, we use a *base*, i.e., a 12-layer Transformer (Vaswani et al., 2017) models. TinyLLAMA has 22 layers and about 1B parameters. BERT-base is more practical than a 24-layer BERT-large and performs at par with BERT-large on MS MARCO and Robust04 (Hofstätter et al., 2020a; Li et al., 2024). In our own experiments, we see that large (24 and more layers) model perform much better on the MS MARCO Passage collection, but we were not able to outperform 12-layer models on the MS MARCO Documents collection. Note that Longformer (Beltagy et al., 2020), BigBird (Zaheer et al., 2020), and DEBERTA base (He et al., 2021), JINA (Günther et al., 2023), and MOSAIC (Portes et al., 2023) all have 12 layers, but a larger embedding matrix.

One training epoch consisted in iterating over all queries and sampling one positive and one negative example with a subsequent computation of a

⁷https://anonymous.4open.science/r/long_doc_rank_model_analysis_v2-78E9/

| Retriever / Ranker | zero-shot transferred | fine-tuned |
|--------------------------------|----------------------------------|------------------------------------|
| Random shuffling of top-100 | 0.052 | 0.052 |
| Retriever (BM25) | 0.207 | 0.207 |
| FirstP (BERT) | 0.016 ^b | 0.090 ^b |
| FirstP (Longformer) | 0.017 ^b | 0.091 ^b |
| FirstP (ELECTRA) | 0.019 ^b | 0.089 ^b |
| FirstP (Big-Bird) | 0.021 ^b | 0.089 ^b |
| FirstP (JINA) | 0.018 ^b | 0.088 ^b |
| FirstP (MOSAIC) | 0.018 ^b | 0.089 ^b |
| FirstP (TinyLLAMA) | 0.020 ^b | 0.079 ^b |
| FirstP (E5-4K) | 0.015 ^{ab} | — |
| AvgP | 0.154 ^{ab} (-48.1%) | 0.365 ^{ab} (+11.4%) |
| MaxP | 0.297 ^b | 0.328 ^b |
| MaxP (ELECTRA) | 0.328 ^b | 0.349 ^b |
| MaxP (DEBERTA) | 0.298 ^b | 0.332 ^b |
| SumP | 0.211 ^{ab} (-28.8%) | 0.327 ^b (-0.4%) |
| CEDR-DRMM | 0.157 ^{ab} (-47.3%) | 0.372 ^{ab} (+13.3%) |
| CEDR-KNRM | 0.055 ^{ab} (-81.5%) | 0.382 ^a (+16.4%) |
| CEDR-PACRR | 0.209 ^{ab} (-29.6%) | 0.393 ^a (+19.9%) |
| Neural Model1 | 0.085 ^{ab} (-71.3%) | 0.396 ^a (+20.6%) |
| PARADE Attn | 0.300 ^b (+1.0%) | 0.337 ^b (+2.8%) |
| PARADE Attn (ELECTRA) | 0.338^b (+3.3%) | 0.354 ^b (+1.6%) |
| PARADE Attn (DEBERTA) | 0.307 ^b (+3.2%) | 0.343 ^b (+3.4%) |
| PARADE Avg | 0.274 ^{ab} (-7.6%) | 0.322 ^b (-1.7%) |
| PARADE Max | 0.291 ^b (-2.1%) | 0.330 ^b (+0.6%) |
| PARADE Transf-RAND-L2 | 0.243 ^a (-18.2%) | 0.419 ^{ab} (+27.7%) |
| P. Transf-RAND-L2 (ELECTRA) | 0.229 ^a (-30.2%) | 0.432^{ab} (+23.8%) |
| PARADE Transf-PRETR-L6 | 0.267 ^{ab} (-10.0%) | 0.413 ^a (+26.0%) |
| P. Transf-PRETR-LATEIR-L6 | 0.244 ^a (-18.0%) | 0.358 ^{ab} (+9.2%) |
| LongP (Longformer) | 0.233 ^a (-21.7%) | 0.399 ^a (+21.7%) |
| LongP (Big-Bird) | 0.126 ^{ab} (-57.4%) | 0.401 ^a (+22.1%) |
| LongP (JINA) | 0.069 ^{ab} (-76.9%) | 0.372 ^{ab} (+13.4%) |
| LongP (MOSAIC) | 0.120 ^{ab} (-59.6%) | 0.397 ^a (+21.2%) |
| LongP (TinyLLAMA) | 0.078 ^{ab} (-73.6%) | 0.397 ^a (+21.1%) |
| LongP (E5-4K) | 0.057 ^{ab} (-80.7%) | N/A (zero-shot only) |
| LongP RankGPT (GPT-4o-mini) | 0.043 ^b | N/A (zero-shot only) |
| LongP RankGPT (Claude-3-haiku) | 0.051 ^b | N/A (zero-shot only) |

In each column we show a relative gain over models' respective *MaxP* baseline. For *LongP* models, the gain is over *MaxP* (BERT). Statistically significant differences from a respective *MaxP* baseline are denoted with the superscript **a**. Statistical significant differences with respect to *Longformer* are denoted with the superscript **b** (p -value < 0.01).

Table 4: Comparison between long-document models and respective *FirstP* (truncation) baselines. Results on MS MARCO FarRelevant.

pairwise margin loss. We used the minibatch size one with gradient accumulation over 16 steps. The learning rates are provided in the model configuration files (in the on-line repository).⁸ We used the AdamW optimizer (Loshchilov and Hutter, 2017) and a constant learning rate with a 20% linear warm-up (Mosbach et al., 2020).

We have learned that—unlike neural *retrievers*—cross-encoding rankers (Nogueira and Cho, 2019) are relatively insensitive to learning rates, their schedules, and the choice of loss functions. We were sometimes able to achieve better results using multiple negatives per query and a listwise margin loss (or cross-entropy). However, the gains were small and not consistent compared to a simple pairwise margin loss used in our work (in fact, using a listwise loss function sometimes lead to overfitting). Note again that this is different from neural *retrievers* where training is difficult without using a listwise loss and/or batch-negatives (Karpukhin et al., 2020; Xiong et al., 2021; Qu et al., 2021; Zerveas et al., 2021; Formal et al., 2021).

For MS MARCO, all models except PARADE-Transf-Pretr-LATEIR-L6 and PARADE-Transf-RAND-L2 were trained for one epoch: Further training did not improve (and sometimes degraded) accuracy. However, PARADE-Transf-RAND-L2 and PARADE-Transf-Pretr-LATEIR-L6 required two-to-three epochs to reach the maximum accuracy. For training using de-biased MS MARCO, we used only one epoch. In the case of Robust04, each model was finetuned for 100 epochs, but all epochs were short, so the overall training and evaluation time was comparable to that of fine-tuning on MS MARCO for a single epoch.

To reproduce our main results, we estimate that one needs about 6400 GPU hours: 6000 hours using NVIDIA A10 (or RTX 3090) with 24 GB of memory and 400 hours using NVIDIA A6000 with 48 GB of memory. A6000 was required only for TinyLLAMA.

From our experience models trained on MS MARCO v2 performed worse on TREC 2021 queries compared to models trained on MS MARCO v1. This may indicate that models somehow learn to distinguish between original MS MARCO v1 documents and newly added ones (which did not have positive judgements in the training sets). As a result, these models are biased

⁸https://anonymous.4open.science/r/long_doc_rank_model_analysis_v2-78E9/.

| Model | MS MARCO dev | 2019 | | TREC DL 2020 | | title | Robust04 description |
|---|----------------------------------|----------------------------|----------------------------------|----------------------------|-----------------------------|----------------------------------|----------------------|
| | | MRR | | NDCG@10 | 2021 | | |
| BM25 | 0.274 | 0.548 | 0.538 | 0.549 | 0.428 | 0.402 | |
| Prior work (FirstP, MaxP), Zhang et al. (Zhang et al., 2021) | | | | | | | |
| FirstP (BERT) | - | - | - | - | 0.449 | 0.510 | |
| MaxP (BERT) | - | - | - | - | 0.477 (+6.2%) | 0.530 (+3.9%) | |
| MaxP (ELECTRA) | - | - | - | - | 0.523 | 0.574 | |
| Prior work (PARADE) Li et al. (Li et al., 2024) | | | | | | | |
| PARADE Attn (ELECTRA) | - | - | - | - | 0.527 | 0.587 | |
| PARADE Max (ELECTRA) | - | 0.679 | 0.613 | - | 0.544 | 0.602 | |
| PARADE Transf-RAND (ELECTRA) | - | 0.650 | 0.601 | - | 0.566 | 0.613 | |
| Our results | | | | | | | |
| FirstP (BERT) | 0.394 | 0.631 | 0.598 | 0.660 | 0.475 | 0.527 | |
| MaxP (BERT) | 0.392 (-0.4%) | 0.648 (+2.6%) | 0.615 (+2.8%) | 0.665 (+0.8%) | 0.488 ^a (+2.6%) | 0.544 ^a (+3.3%) | |
| PARADE Attn | 0.416 ^a (+5.5%) | 0.647 (+2.5%) | 0.626 ^a (+4.6%) | 0.677 (+2.5%) | 0.503 ^a (+5.7%) | 0.556 ^a (+5.6%) | |
| FirstP (ELECTRA) | 0.417 | 0.652 | 0.642 | 0.686 | 0.492 | 0.552 | |
| MaxP (ELECTRA) | 0.414 (-0.6%) | 0.659 (+1.0%) | 0.630 (-1.9%) | 0.683 (-0.5%) | 0.502 (+2.0%) | 0.563 (+2.1%) | |
| PARADE Attn (ELECTRA) | 0.431^a (+3.3%) | 0.675 ^a (+3.5%) | 0.653 (+1.8%) | 0.705 (+2.8%) | 0.523 ^a (+6.4%) | 0.581 ^a (+5.3%) | |
| FirstP (DEBERTA) | 0.415 | 0.675 | 0.629 | 0.702 | 0.534 | 0.596 | |
| MaxP (DEBERTA) | 0.402 (-3.2%) | 0.679 (+0.6%) | 0.620 (-1.4%) | 0.705 (+0.4%) | 0.535 (+0.2%) | 0.609 (+2.2%) | |
| PARADE Attn (DEBERTA) | 0.422 ^a (+1.6%) | 0.685 (+1.4%) | 0.659^a (+4.8%) | 0.713 (+1.4%) | 0.549 ^a (+2.9%) | 0.615^a (+3.2%) | |
| FirstP (Longformer) | 0.404 | 0.657 | 0.616 | 0.654 | 0.483 | 0.540 | |
| LongP (Longformer) | 0.412 ^a (+1.9%) | 0.676 ^a (+2.9%) | 0.628 (+2.0%) | 0.693 ^a (+6.0%) | 0.500 ^a (+3.6%) | 0.568 ^a (+5.1%) | |
| FirstP (Big-Bird) | 0.408 | 0.663 | 0.620 | 0.679 | 0.507 | 0.560 | |
| LongP (Big-Bird) | 0.397 ^a (-2.9%) | 0.655 (-1.1%) | 0.618 (-0.3%) | 0.675 (-0.5%) | 0.452 ^a (-10.9%) | 0.477 ^a (-14.9%) | |
| FirstP (JINA) | 0.422 | 0.658 | 0.618 | 0.679 | 0.488 | 0.532 | |
| LongP (JINA) | 0.416 ^a (-1.5%) | 0.670 ^a (+1.8%) | 0.632 (+2.1%) | 0.689 (+1.4%) | 0.503 ^a (+2.9%) | 0.558 ^a (+4.9%) | |
| FirstP (MOSAIC) | 0.423 | 0.654 | 0.607 | 0.662 | 0.453 | 0.538 | |
| LongP (MOSAIC) | 0.421 (-0.4%) | 0.660 (+0.9%) | 0.630 ^a (+3.7%) | 0.694 ^a (+4.9%) | 0.456 (+0.6%) | 0.570 ^a (+6.0%) | |

In each column we show a relative gain over model’s respective *FirstP* baseline: The last column shows the average relative gain over *FirstP*. Best numbers are in **bold**: Our results are averaged over three seeds (but not necessarily prior art). Statistical significant differences with respect to this baseline are denoted using the superscript superscript **a**. *p*-value threshold is 0.01 for an MS MARCO development collection and 0.05 otherwise.

Table 5: Comparison between long-document models and respective *FirstP* (truncation) baselines as well as to *prior art*. Results for MS MARCO, TREC DL, and Robust04.

and tend to not rank these new documents well even when they are considered to be relevant by NIST assessors. For this reason, we used MS MARCO v2 data in a zero-shot transfer mode where ranking models trained on MS MARCO v1 are evaluated on TREC DL 2021 queries.

A.1.3 Miscellaneous Notes

To enable efficient training and evaluation of the large number of models, for Robust04 and original MS MARCO documents were truncated to have at most 1431 BERT tokens. In § A.2 (see Table 6) we show that for our top-performing model PARADE Attention (Li et al., 2024) using a larger number of chunks only marginally improves outcomes. Depending on a dataset, the highest accuracy is achieved using either three or four chunks. However, for training on de-biased MS MARCO, the truncation threshold is much higher: 8109 tokens.

For *SplitP* approaches, queries were padded to

32 BERT tokens with padding being masked out during training (longer queries were truncated). For *SplitP* models with greedy partitioning into disjoint chunks, long document were split into at most three chunks containing 477 document tokens (each concatenated with up to 32 query tokens plus three special tokens).

We evaluated 20+ models, but we had to exclude two LongT5 variants (Guo et al., 2022) and RoFormer (with ROPE embeddings) (Su et al., 2024) due to poor convergence and/or crashes. Specifically, even after 10 epochs of training LongT5 models were $\approx 10\%$ less accurate than BERT-base *FirstP* trained for one epoch. Given the uncertainty regarding the possible convergence of models as well as the need to train these for three epochs, we have to abandon this experiment as overly expensive. RoFormer models were failing due to CUDA errors when the context length exceeded 512: We were not able to resolve this issue.

For bias-mitigation experiments, for several rea-

1363
1364
1365
1366
1367
1368
1369
1370
1371
1372
1373
1374
1375
1376
1377
1378
1379
1380
1381
1382

1383
1384
1385
1386
1387
1388
1389
1390
1391
1392
1393
1394
1395
1396
1397
1398
1399
1400
1401
1402
1403

| Retriever / Ranker | MS MARCO dev | TREC DL (2019-2021) | title | Robust04 description | Avg. gain Over FirstP |
|------------------------------------|----------------------------------|----------------------------------|----------------------------------|----------------------------------|-----------------------|
| | MRR | NDCG@10 | | NDCG@20 | |
| BM25 | 0.274 | 0.545 | 0.428 | 0.402 | - |
| Retriever (if different from BM25) | 0.312 | 0.629 | - | - | - |
| PARADE Attn (1 chunk) | 0.401 | 0.637 | 0.476 | 0.527 | - |
| PARADE Attn (2 chunks) | 0.408 ^a (+1.8%) | 0.653 ^a (+2.7%) | 0.499 ^a (+4.9%) | 0.544 ^a (+3.3%) | +3.2% |
| PARADE Attn (3 chunks) | 0.406 ^a (+1.3%) | 0.648 ^a (+1.7%) | 0.505^a (+6.1%) | 0.557 ^a (+5.7%) | +3.7% |
| PARADE Attn (4 chunks) | 0.412^a (+2.9%) | 0.654^a (+2.7%) | 0.504 ^a (+5.9%) | 0.558^a (+5.9%) | +4.3% |
| PARADE Attn (5 chunks) | 0.409 ^a (+2.0%) | 0.652 ^a (+2.4%) | 0.502 ^a (+5.6%) | 0.556 ^a (+5.5%) | +3.9% |
| PARADE Attn (6 chunks) | 0.411 ^a (+2.4%) | 0.653 ^a (+2.6%) | 0.504 ^a (+5.9%) | 0.554 ^a (+5.2%) | +4.0% |

Table 6: Effectiveness of the PARADE Attention model for different input truncation thresholds. **Results for MS MARCO, TREC DL, and Robust04.**

sons, we used only a subset of models. First, we had to exclude all *LongP* models since none of them supported a context longer than 8192 tokens. In contrast, in this experiment we trained our chunk-and-aggregate tokens up to the length of 8109 and then extrapolated to rank documents up to 32768 tokens long. Second, we chose representative models with vastly different generalization properties. MaxP and PARADE Attention models performed well on MS MARCO FarRelevant in the zero-shot setting, but did not benefit much from in-domain fine-tuning. PARADE Transformer MRR dropped from 0.433 to 0.229 in the zero-shot setting, but increased up to 0.432 after in-domain fine-tuning. CEDR-KNRM also benefited a lot from fine-tuning on MS MARCO FarRelevant, but its zero-shot performance was at the level of random-baseline.

A.2 Varying the Number of Chunks

To understand if truncating input to have at most 1431 BERT tokens negatively affected model performance, we carried out an ablation study where one of the top-performing models was trained and evaluated using inputs of varying maximum lengths. To this end we used PARADE Attention with the number of input chunks varying from one to six. In that same number of chunks was used during training and evaluation, i.e., we had to carry out six experiments. Similar to our main experiments, we trained each model using three seeds. We carried out this ablation experiment using our MS MARCO and Robust04 datasets.

The results are presented in Table 6: We can see that—depending on the dataset—three or four input chunks are optimal. However, the additional gains over the *FirstP* baseline are at most 0.6% when averaged over all test sets.

Gao and Callan 2022 carried out a similar abla-

tion using ClueWeb09: Increasing the number of input chunks from three to six lead to only about 2.3% relative improvement in NDCG@20. However, even this modest gain could have been slightly inflated due to model not being trained *directly* on shorter inputs. Indeed, truncation of an input for a six-chunk model to one chunk is potentially less effective than training and evaluating the model using one-chunk data.

A.3 Backbone Selection for *SplitP* Models and Prior Art Comparison

A.3.1 Choice of a Backbone

To understand if using BERT-base as backbone model for various *SplitP* (i.e., chunk-and-aggregate) approaches diminished models’ ability to process and understand long contexts, we carried out a focused comparison of several backbone models, including ELECTRA (Clark et al., 2020) and DEBERTA (He et al., 2021). To this end, we used two methods: PARADE (Li et al., 2024) Attention and *MaxP*. PARADE Attention model achieved the largest average gain over *FirstP* in our main experiments (see Table 1), whereas *MaxP* models were extensively benchmarked in the past (Li et al., 2024; Dai and Callan, 2019; Zhang et al., 2021). Although prior work found ELECTRA to be a better backbone model in terms of *absolute* accuracy (Li et al., 2024; Zhang et al., 2021), we found no systematic evaluation of the relationship between a backbone model and achievable *FirstP* gains.

Results in Tables 5 and 1 confirm overall superiority of both ELECTRA and DEBERTA over BERT-base. In that, DEBERTA models are nearly always more effective compared to ELECTRA models with biggest differences on Robust04. However, their *relative* effectiveness with respect

| Model | MS MARCO dev | | TREC DL 2019-2021 | |
|---------------------------------|----------------------------------|----------------------------|----------------------------|----------------------------|
| | MRR | NDCG@10 | P@10 | MAP |
| BM25 | 0.274 | 0.545 | 0.636 | 0.282 |
| Retriever | 0.312 | 0.629 | 0.720 | 0.321 |
| FirstP (BERT) | 0.394 | 0.632 | 0.712 | 0.311 |
| FirstP (Longformer) | 0.404 | 0.643 | 0.722 | 0.317 |
| FirstP (ELECTRA) | 0.417 | 0.662 | 0.734 | 0.320 |
| FirstP (DEBERTA) | 0.415 | 0.672 | 0.741 | 0.327 |
| FirstP (Big-Bird) | 0.408 | 0.656 | 0.727 | 0.321 |
| FirstP (JINA) | 0.422 | 0.654 | 0.728 | 0.320 |
| FirstP (MOSAIC) | 0.423 | 0.643 | 0.726 | 0.316 |
| FirstP (TinyLLAMA) | 0.395 | 0.615 | 0.692 | 0.301 |
| FirstP (E5) | 0.380 | 0.641 | 0.722 | 0.317 |
| FirstP RankGPT (OpenAI) | — | 0.708 | 0.790 | 0.352 |
| FirstP RankGPT (Anthropic) | — | 0.703 | 0.776 | 0.347 |
| AvgP | 0.389 (-1.3%) | 0.642 (+1.5%) | 0.717 (+0.7%) | 0.317 ^a (+2.0%) |
| MaxP | 0.392 (-0.4%) | 0.644 ^a (+1.9%) | 0.723 (+1.5%) | 0.322 ^a (+3.7%) |
| MaxP (ELECTRA) | 0.414 (-0.6%) | 0.659 (-0.5%) | 0.745 (+1.5%) | 0.326 (+2.1%) |
| MaxP (DEBERTA) | 0.402 ^a (-3.2%) | 0.671 (-0.1%) | 0.746 (+0.7%) | 0.335 ^a (+2.5%) |
| SumP | 0.390 (-1.0%) | 0.639 (+1.0%) | 0.715 (+0.4%) | 0.319 ^a (+2.6%) |
| CEDR-DRMM | 0.385 ^a (-2.3%) | 0.629 (-0.5%) | 0.708 (-0.5%) | 0.313 (+0.6%) |
| CEDR-KNRM | 0.379 ^a (-3.8%) | 0.630 (-0.3%) | 0.711 (-0.1%) | 0.313 (+0.8%) |
| CEDR-PACRR | 0.395 (+0.3%) | 0.643 ^a (+1.6%) | 0.719 (+0.9%) | 0.320 ^a (+2.9%) |
| Neural Model1 | 0.398 (+0.9%) | 0.650 ^a (+2.8%) | 0.723 ^a (+1.5%) | 0.323 ^a (+3.9%) |
| PARADE Attn | 0.416 ^a (+5.5%) | 0.652 ^a (+3.1%) | 0.728 ^a (+2.2%) | 0.324 ^a (+4.2%) |
| PARADE Attn (ELECTRA) | 0.431 ^a (+3.3%) | 0.680 ^a (+2.7%) | 0.763 ^a (+3.9%) | 0.335 ^a (+4.9%) |
| PARADE Attn (DEBERTA) | 0.422 ^a (+1.6%) | 0.688 ^a (+2.4%) | 0.763 ^a (+3.0%) | 0.339 ^a (+3.9%) |
| PARADE Avg | 0.392 (-0.6%) | 0.646 ^a (+2.1%) | 0.715 (+0.4%) | 0.317 ^a (+2.1%) |
| PARADE Max | 0.405 ^a (+2.7%) | 0.655 ^a (+3.5%) | 0.733 ^a (+2.9%) | 0.324 ^a (+4.1%) |
| PARADE Transf-RAND-L2 | 0.419 ^a (+6.3%) | 0.655 ^a (+3.6%) | 0.734 ^a (+3.1%) | 0.326 ^a (+5.0%) |
| PARADE Transf-RAND-L2 (ELECTRA) | 0.433^a (+3.9%) | 0.670 (+1.2%) | 0.747 (+1.8%) | 0.327 (+2.2%) |
| PARADE Transf-PRETR-L6 | 0.402 ^a (+1.9%) | 0.643 (+1.6%) | 0.717 (+0.8%) | 0.322 ^a (+3.6%) |
| PARADE Transf-PRETR-LATEIR-L6 | 0.398 (+1.1%) | 0.626 (-0.9%) | 0.707 (-0.7%) | 0.307 (-1.1%) |
| LongP (Longformer) | 0.412 ^a (+1.9%) | 0.668 ^a (+3.9%) | 0.752 ^a (+4.1%) | 0.333 ^a (+5.1%) |
| LongP (Big-Bird) | 0.397 ^a (-2.9%) | 0.651 (-0.7%) | 0.726 (-0.2%) | 0.322 (+0.3%) |
| LongP (JINA) | 0.416 ^a (-1.5%) | 0.665 ^a (+1.7%) | 0.742 ^a (+2.0%) | 0.328 ^a (+2.4%) |
| LongP (MOSAIC) | 0.421 (-0.4%) | 0.664 ^a (+3.3%) | 0.740 ^a (+1.9%) | 0.327 ^a (+3.7%) |
| LongP (TinyLLAMA) | 0.402 ^a (+1.7%) | 0.608 (-1.1%) | 0.692 (+0.0%) | 0.306 (+1.6%) |
| LongP (E5) | 0.353 ^a (-7.1%) | 0.649 (+1.3%) | 0.724 (+0.3%) | 0.323 (+1.8%) |
| LongP RankGPT (OpenAI) | — | 0.706 (-0.3%) | 0.783 (-1.0%) | 0.350 (-0.7%) |
| LongP RankGPT (Anthropic) | — | 0.707 (+0.5%) | 0.780 (+0.5%) | 0.348 (+0.4%) |

In each column we show a relative gain with respect model's respective *FirstP* baseline: The last column shows the average relative gain of *FirstP*. Best numbers are in **bold**: Results are averaged over three seeds. Unless specified explicitly, the backbone is **BERT-base**.

Statistical significant differences with respect to this baseline are denoted using the superscript superscript **a**. *p*-value threshold is 0.01 for an MS MARCO development collection and 0.05 otherwise.

E5-models were used only in the zero-shot model, i.e., without fine-tuning.

Table 7: Comparison between long-document models and respective FirstP (truncation) baselines. Results for MS MARCO and TREC DL.

| Model | NDCG@20 | P@20 | MAP | NDCG@20 | P@20 | MAP |
|-------------------------------|----------------------------------|----------------------------------|----------------------------------|----------------------------------|----------------------------------|----------------------------------|
| Retriever (BM25) | 0.428 | 0.365 | 0.255 | 0.402 | 0.334 | 0.240 |
| FirstP (BERT) | 0.475 | 0.405 | 0.277 | 0.527 | 0.447 | 0.303 |
| FirstP (Longformer) | 0.483 | 0.413 | 0.277 | 0.540 | 0.454 | 0.307 |
| FirstP (ELECTRA) | 0.492 | 0.424 | 0.294 | 0.552 | 0.465 | 0.320 |
| FirstP (DEBERTA) | 0.534 | 0.459 | 0.319 | 0.596 | 0.503 | 0.350 |
| FirstP (Big-Bird) | 0.507 | 0.435 | 0.300 | 0.560 | 0.473 | 0.325 |
| FirstP (JINA) | 0.488 | 0.421 | 0.287 | 0.532 | 0.450 | 0.305 |
| FirstP (MOSAIC) | 0.453 | 0.390 | 0.266 | 0.538 | 0.455 | 0.310 |
| FirstP (TinyLLAMA) | 0.431 | 0.370 | 0.246 | 0.473 | 0.398 | 0.262 |
| FirstP (E5-4K) | 0.438 | 0.371 | 0.247 | 0.429 | 0.355 | 0.234 |
| FirstP RankGPT (OpenAI) | — | — | — | 0.562 | 0.456 | 0.280 |
| FirstP RankGPT (Anthropic) | — | — | — | 0.541 | 0.446 | 0.268 |
| AvgP | 0.478 (+0.5%) | 0.411 (+1.6%) | 0.292 ^a (+5.4%) | 0.531 (+0.9%) | 0.451 (+1.0%) | 0.324 ^a (+6.7%) |
| MaxP | 0.488 ^a (+2.6%) | 0.425 ^a (+5.1%) | 0.306 ^a (+10.6%) | 0.544 ^a (+3.3%) | 0.467 ^a (+4.5%) | 0.338 ^a (+11.5%) |
| MaxP (ELECTRA) | 0.502 (+2.0%) | 0.441 ^a (+3.9%) | 0.319 ^a (+8.3%) | 0.563 (+2.1%) | 0.483 ^a (+4.0%) | 0.350 ^a (+9.3%) |
| MaxP (DEBERTA) | 0.535 (+0.2%) | 0.464 (+1.2%) | 0.340 ^a (+6.7%) | 0.609 ^a (+2.2%) | 0.519 ^a (+3.2%) | 0.378 ^a (+7.9%) |
| SumP | 0.486 (+2.2%) | 0.418 ^a (+3.4%) | 0.305 ^a (+10.2%) | 0.538 (+2.1%) | 0.461 ^a (+3.1%) | 0.337 ^a (+11.1%) |
| CEDR-DRMM | 0.466 (-2.0%) | 0.403 (-0.4%) | 0.287 ^a (+3.8%) | 0.533 (+1.3%) | 0.458 ^a (+2.5%) | 0.326 ^a (+7.6%) |
| CEDR-KNRM | 0.483 (+1.7%) | 0.413 (+1.9%) | 0.291 ^a (+5.1%) | 0.535 (+1.7%) | 0.456 (+2.0%) | 0.324 ^a (+6.8%) |
| CEDR-PACRR | 0.496 ^a (+4.3%) | 0.426 ^a (+5.3%) | 0.307 ^a (+11.0%) | 0.549 ^a (+4.2%) | 0.466 ^a (+4.4%) | 0.337 ^a (+11.2%) |
| Neural Model1 | 0.484 (+1.8%) | 0.417 ^a (+3.1%) | 0.298 ^a (+7.7%) | 0.537 (+1.9%) | 0.459 ^a (+2.6%) | 0.330 ^a (+8.8%) |
| PARADE Attn | 0.503 ^a (+5.7%) | 0.433 ^a (+6.9%) | 0.311 ^a (+12.4%) | 0.556 ^a (+5.6%) | 0.476 ^a (+6.5%) | 0.344 ^a (+13.3%) |
| PARADE Attn (ELECTRA) | 0.523 ^a (+6.4%) | 0.456 ^a (+7.4%) | 0.329 ^a (+11.7%) | 0.581 ^a (+5.3%) | 0.495 ^a (+6.5%) | 0.358 ^a (+11.9%) |
| PARADE Attn (DEBERTA) | 0.549^a (+2.9%) | 0.475^a (+3.6%) | 0.346^a (+8.7%) | 0.615^a (+3.2%) | 0.522^a (+3.8%) | 0.383^a (+9.4%) |
| PARADE Avg | 0.483 (+1.5%) | 0.412 (+1.8%) | 0.291 ^a (+5.2%) | 0.534 (+1.5%) | 0.457 (+2.4%) | 0.318 ^a (+4.7%) |
| PARADE Max | 0.489 ^a (+2.8%) | 0.420 ^a (+3.8%) | 0.306 ^a (+10.8%) | 0.548 ^a (+4.0%) | 0.470 ^a (+5.3%) | 0.337 ^a (+11.0%) |
| PARADE Transf-RAND-L2 | 0.488 ^a (+2.8%) | 0.423 ^a (+4.6%) | 0.303 ^a (+9.7%) | 0.548 ^a (+4.1%) | 0.469 ^a (+5.0%) | 0.338 ^a (+11.6%) |
| PAR. Transf-RAND-L2 (ELECTRA) | 0.523 ^a (+6.3%) | 0.454 ^a (+6.9%) | 0.330 ^a (+12.2%) | 0.574 ^a (+3.9%) | 0.488 ^a (+5.0%) | 0.354 ^a (+10.6%) |
| PARADE Transf-PRETR-L6 | 0.494 ^a (+4.0%) | 0.426 ^a (+5.3%) | 0.308 ^a (+11.5%) | 0.554 ^a (+5.1%) | 0.474 ^a (+6.1%) | 0.346 ^a (+14.1%) |
| PAR. Transf-PRETR-LATEIR-L6 | 0.450 ^a (-5.2%) | 0.389 ^a (-3.9%) | 0.277 (+0.3%) | 0.501 ^a (-4.9%) | 0.423 ^a (-5.3%) | 0.302 (-0.5%) |
| LongP (Longformer) | 0.500 ^a (+3.6%) | 0.435 ^a (+5.3%) | 0.309 ^a (+11.5%) | 0.568 ^a (+5.1%) | 0.482 ^a (+6.1%) | 0.347 ^a (+12.9%) |
| LongP (Big-Bird) | 0.452 ^a (-10.9%) | 0.389 ^a (-10.7%) | 0.274 ^a (-8.8%) | 0.477 ^a (-14.9%) | 0.400 ^a (-15.5%) | 0.279 ^a (-14.2%) |
| LongP (JINA) | 0.503 ^a (+2.9%) | 0.434 ^a (+3.1%) | 0.309 ^a (+7.5%) | 0.558 ^a (+4.9%) | 0.473 ^a (+5.2%) | 0.335 ^a (+9.7%) |
| LongP (MOSAIC) | 0.456 (+0.6%) | 0.393 (+0.8%) | 0.280 ^a (+5.3%) | 0.570 ^a (+6.0%) | 0.484 ^a (+6.3%) | 0.350 ^a (+13.0%) |
| LongP (TinyLLAMA) | 0.452 ^a (+4.8%) | 0.396 ^a (+6.9%) | 0.267 ^a (+8.7%) | 0.505 ^a (+6.7%) | 0.428 ^a (+7.6%) | 0.297 ^a (+13.3%) |
| LongP (E5-4K) | 0.439 (+0.1%) | 0.375 (+1.0%) | 0.250 (+1.3%) | 0.434 (+1.1%) | 0.360 (+1.6%) | 0.241 ^a (+2.9%) |
| LongP RankGPT (OpenAI) | — | — | — | 0.562 (+0.0%) | 0.456 (-0.0%) | 0.281 (+0.3%) |
| LongP RankGPT (Anthropic) | — | — | — | 0.538 (-0.6%) | 0.445 (-0.2%) | 0.268 (-0.0%) |

In each column we show a relative gain with respect model's respective *FirstP* baseline: The last column shows the average relative gain of *FirstP*. Best numbers are in **bold**: Results are averaged over three seeds. Unless specified explicitly, the backbone is **BERT-base**.

Statistical significant differences with respect to this baseline are denoted using the superscript superscript **a**. *p*-value threshold is 0.05. E5-models were used only in the zero-shot model, i.e., without fine-tuning.

Table 8: Comparison between long-document models and respective FirstP (truncation) baselines. Results for Robust04.

to their respective *FirstP* baselines does not exceed that of BERT-base. The same is true for *LongP* models. Except Longformer they performed equally or worse compared to *FirstP* on 8 test sets out of 18. Moreover, all *LongP* models achieved lower average gains over *FirstP* (see the last column in Table 1). We conclude that to measure capabilities of chunk-and-aggregate model to understand and incorporate long context, it appears to be *beneficial* to use BERT-base instead of ELECTRA or DEBERTA.

Finally, we would like to note that on standard benchmarks Big-Bird’s (Zaheer et al., 2020) *FirstP* version always outperforms its *LongP* version (sometimes by as much as 10-15%), which seems to be puzzling. We noticed, however, that for shorter inputs, the model turns off sparse attention and prints the respective warning. Thus, we hypothesize that it is the use of sparse attention that causes this degradation. In contrast, the sparse attention implementation of the Longformer (Beltagy et al., 2020) does not exhibit such a degradation (although with Longformer, not all attention is sparse: query-to-document attention is full). Despite Big-Bird underperforms on standard benchmarks, it still does well on MS MARCO FarRelevant after fine-tuning (see Table 4).

A.4 Efficiency Evaluation

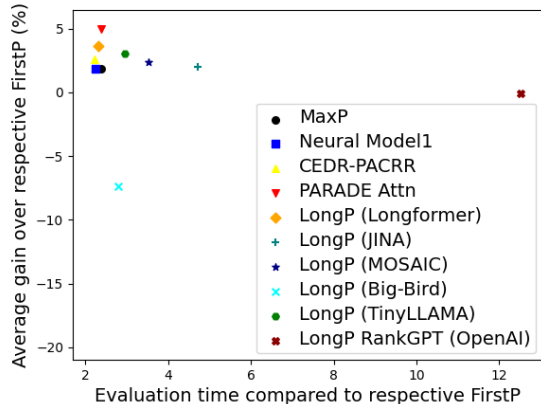


Figure 3: **Efficiency of long-document models vs respective (truncation) *FirstP* baselines.** The figure shows an average relative gain (in %) vs. relative increase in run-time compared to *respective FirstP* baselines on MS MARCO, TREC DL 2019-2021, and Robust04 (for a representative subset of models). Except LongP RankGPT, *LongP* models truncate documents to be at most 1431 tokens. There is no truncation for RankGPT.

From the efficiency-effectiveness plot in Fig. 3, we can see that all long-document models are at least $2\times$ slower than respective *FirstP* baselines. The biggest average gain of merely 5% is achieved by the PARADE Attn model (with a BERT-base backbone) at the cost of being $2.5\times$ slower than its *FirstP* baseline. All *LongP* models are even slower and show less improvement. Given such small benefits at the cost of a substantial slow-down, one could question practicality of such models and suggest using *FirstP* variants instead.

A.4.1 Comparison to Prior Art

We also use Table 5 to compare with prior art. We generally reproduce prior art, in particular, experiments by Li et al. 2024, who invented PARADE models. Our ELECTRA-based models achieve higher NDCG@10 on TREC DL 2019-2020 and PARADE Attention models come very close, but they are about 3-5% worse compared to their PARADE Transformer on Robust04. At the same time, our DEBERTA-based PARADE Attention model achieves similar NDCG@20 scores.

Note that one should not expect identical results due to differences in training regimes and candidate generators. In particular, in the case of Robust04, Li et al. 2024 use RM3 (BM25 with a pseudo-relevance feedback (Jaleel et al., 2004)), which is more effective than BM25 (Robertson, 2004) (which we use on Robust04).

Another important comparison point is Robust04 results by Zhang et al. 2021 who were able to reproduce original *MaxP* results by Dai and Callan 2019, which used BERT-base as a backbone. In addition, they experimented with ELECTRA models “pre-finetuned” on MS MARCO. When comparing BERT-base results, Zhang et al. 2021 have the maximum relative gain of 6.6% compared to ours 3.3%. However, in absolute terms we got higher NDCG@20 for both *FirstP* and *MaxP*. Their *MaxP* (ELECTRA) has comparable performance to ours on TREC DL 2019-2020, but it is 2-4% better on Robust04. In turn, our *MaxP* (DEBERTA) is better by 2-6%. Although we do not always match prior art using the same backbone models, we generally match or outperform prior results, which, we believe, boosts the trustworthiness of our experiments.

A.5 Additional Experimental Results

In this section we provide links for additional experimental results. In particular, we compute ad-

ditional effectiveness metrics for MS MARCO, TREC DL, and Robust04. MS MARCO and TREC DL results are shown in Table 7. Robust04 datasets are presented and Table 8. Furthermore, we provide detailed results for MS MARCO FarRelevant in Table 4. Evaluation results of rankers trained on de-biased data and tested on short-document collections can be found in Table 3.

B Additional Dataset Details

B.1 Summary Dataset Statistics

| data set | # of documents | average # of BERT tokens per document |
|----------------------------|----------------|---------------------------------------|
| Long-document collections | | |
| MS MARCO doc. v1 | 3.2M | 1.4K |
| MS MARCO doc. v2 | 12M | 2K |
| Robust04 | 0.5M | 0.6K |
| MS MARCO FarRelevant | 0.53M | 1.1K |
| Needle (LongEmbed) | 0.8K | variable-length |
| Passkey (LongEmbed) | 0.8K | variable-length |
| Short-document collections | | |
| MS MARCO pass. v1 | 8.8M | 75 |
| Natural Questions (BEIR) | 2.7M | 107 |

LONGEMBED subsets each have 16 subsets of documents whose lengths vary from (approximately) 256 to 32768 tokens.

Table 9: Document Statistics

| | # of queries | avg. # of BERT tokens | avg. # of pos. judgements |
|--------------------------|--------------|-----------------------|---------------------------|
| MS MARCO doc. v1 | | | |
| MS MARCO doc. train | 352K | 7 | 1 |
| MS MARCO doc. dev | 5193 | 7 | 1 |
| TREC DL 2019 | 43 | 7 | 153.4 |
| TREC DL 2020 | 45 | 7.4 | 39.3 |
| MS MARCO v2 | | | |
| TREC DL 2021 | 57 | 9.8 | 143.9 |
| Robust04 | | | |
| title | 250 | 3.6 | 69.6 |
| description | 250 | 18.7 | 69.6 |
| MS MARCO FarRelevant | | | |
| train | 50K | 7.0 | 1 |
| test | 1K | 7.0 | 1 |
| LongEmbed | | | |
| Needle | 800 | 13.0 | 1 |
| Passkey | 800 | 9.7 | 1 |
| Natural Questions (BEIR) | | | |
| all queries | 3452 | 9.9 | 1.2 |
| MS MARCO pass. v1 | | | |
| TREC DL 2019 | 43 | 7 | 95.4 |
| TREC DL 2020 | 54 | 7.2 | 66.8 |

Table 10: Query Statistics

Summary query and dataset statistics is given in Tables 9 and 10. Please, note that in the case of MS MARCO FarRelevant, we created about 500K training and 7K testing queries, but to reduce experimentation cost we ended up using only 50K and 1K, respectively.

B.2 MS MARCO FarRelevant Creation Algorithm

The MS MARCO FarRelevant dataset was created as follows: Assume that C_t is the number of tokens in the passage:

- Select randomly a document length between $512 + C_t$ and 1431;
- Using rejection sampling, obtain K_1 non-relevant samples such that their *total* length exceeds 512, but the length of $K_1 - 1$ first samples is at most 512.
- Using the same approach, sample another $K_2 + 1$ samples such that the total length of K_2 samples is at most $1431 - C_t$, but the total length of $K_2 + 1$ samples exceeds this value.
- Discard the last sampled passage and randomly mix the remaining K_2 non-relevant passages with a single relevant passage.
- Finally, append the resulting string to the concatenation of the first K_1 non-relevant passages.

B.3 Comparison of FarRelevant and Synthetic Data from LongEmbed

Our synthetic data consists of two subsets Needle and Passkey from LongEmbed collection (Zhu et al., 2024) and our newly created MS MARCO FarRelevant dataset. The datasets can be seen a variant of a needle-in-the-haystack benchmark (Saad-Falcon et al., 2024; Zhu et al., 2024) and they share a common limitation: the resulting documents are constructed by combining pieces of text in a purely mechanical fashion and do not represent natural documents. In this section, we describe Needle and Passkey in more detail and compare them to our proposed collection MS MARCO FarRelevant, which—we believe—offers several practical advantages despite also being synthetic.

The needle subset is created by taking a single document (a Paul Graham essay on taste⁹), truncating it to generate 16 buckets of varying lengths

⁹<https://www.paulgraham.com/goodtaste.html>

Aaron Swartz created a scraped feed of the essays page. November 2021 (This essay is derived from a talk at the Cambridge Union.) When I was a kid, I'd have said there wasn't. My father told me so. Some people like some things, and other people like other things, and who's to say who's right? It seemed so obvious that there was no such thing as good taste that it was only through indirect evidence that I realized my father was wrong.

The novel "The Lord of the Rings" was written by Tolkien and published in the mid-20th century. And that's what I'm going to give you here: a proof by reductio ad absurdum. If we start from the premise that there's no such thing as good taste, we end up with conclusions that are obviously false, and therefore the premise must be wrong. We'd better start by saying what good taste is. There's a narrow sense in which it refers to aesthetic judgements and a broader one in which it refers to preferences of any kind. The strongest proof would be to show that taste exists in the

Figure 4: A sample relevant document for the Needle collection. The query/question is: "Who wrote the novel "The Lord of the Rings" and when was it published?". The answer-bearing sentence is marked by bold font.

The grass is green. The sky is blue. The sun is yellow. Here we go. There and back again. The grass is green. The sky is blue. The sun is yellow. Here we go. There and back again. The grass is green. The sky is blue. The sun is yellow. Here we go. There and back again. The grass is green. The sky is blue. The sun is yellow. Here we go. There and back again. Joyce Jenkins's pass key is **44349**. Remember it. **44349** is the pass key for Joyce Jenkins. The grass is green. The sky is blue. The sun is yellow. Here we go. There and back again. The grass is green. The sky is blue. The sun is yellow. Here we go. There and back again. The grass is green. The sky is blue. The sun is yellow. Here we go. There and back again. The grass is green. The sky is blue. The sun is yellow. Here we go. There and back again. The grass is green. The sky is blue. The sun is yellow. Here we go.

Figure 5: A sample relevant document for the Passkey collection. The query/question is: "what is the passkey for Joyce Jenkins?". The answer-bearing sentence is marked by bold font.

Andhra Pradesh Airports make an easy access for tourists visiting the state. This huge state has many airports, which serves the needs of both tourists and residents commuting to different parts in its large expanse. However, Hyderabad Airport is the major as well as the only international airport of Andhra Pradesh. Hyderabad, a major IT hub of India, boasts of the sixth busiest airport in India. Keeping the rush of passengers in mind, the Government is planning to establish another airport in Hyderabad.

In contrast, traditional English Longbow shooters step into the bow, exerting force with both the bow arm and the string hand arm simultaneously, especially when using bows having draw weights from 100 lbs to over 175 lbs. Heavily stacked traditional bows (recurves, long bows, and the like) are released immediately upon reaching full draw at maximum weight, whereas compound bows reach their maximum weight around the last inch and a half, dropping holding weight significantly at full draw. The Oreo Biscuit was first developed and produced by the National Biscuit Company (today known as Nabisco) in 1912 at its Chelsea, Manhattan factory in the current-day Chelsea Market complex, located on Ninth Avenue between 15th and 16th Streets. Today, this same block of Ninth Avenue is known as Oreo Way..

It's possible to take a day trip to the Bahamas by ferry. In some cases, less than it would cost to fly. The high-speed Balearia Bahamas Express travels from Fort Lauderdale to the city of Freeport on Grand Bahama, one of many Bahamian islands with British roots. It's roughly the distance from Philadelphia to New York. Prepare for a long day. In some cases, less than it would cost to fly. The high-speed Balearia Bahamas Express travels from Fort Lauderdale to the city of Freeport on Grand Bahama, one of many Bahamian islands with British roots. It's roughly the distance from Philadelphia to New York.

I was 17 when I took Bactrim for a UTI, I was a month away from turning 18 and was given this because another antibiotic would have more side effects I was told. I took it for 5 days and became horribly sick from a nasty cold and was told to stop Bactrim and to take Z Pac instead for 5 days.

Cases When Medicare Does NOT Automatically Start for You Medicare will NOT automatically start when you turn 65 if you're not receiving Social Security Benefits or Railroad Retirement Benefits for at least 4 months prior to your 65th birthday. You wanted to know how you can feel on your belly that you're pregnant. And actually this a pretty hard thing to do. There are better ways to find out if you're pregnant or not. For example, if you ever miss a period, the best thing to do is to take a home pregnancy test, because that's the first sign of pregnancy. And if it's positive, ...here are better ways to find out if you're pregnant or not. For example, if you ever miss a period, the best thing to do is to take a home pregnancy test, because that's the first sign of pregnancy.

1 Whisk light soy sauce, dark soy sauce, red wine vinegar, chili oil, ginger, sugar, garlic, and green onion together in a bowl; pour into a sealable container, seal, and refrigerate 1 hour. See how to make a simple sweet-and-sour peach sauce. See how easy and delicious it is to make horseradish sauce from scratch.

Here you'll find a number of Kentucky facts including the state history at a glance; Kentucky state facts such as the location of the state capital, city populations, geography and natural resources; Information on Kentucky' government, symbols and traditions; and even a list of famous Kentuckians.

Confidence votes 193. Replacing a car window usually cost around \$300 give or take based upon where you live, what options your car glass needs and what type of car you drive. Additionally, you can save money if you can repair your car glass instead of completely replacing it. However, if the window is completely shattered this will not be an option.

Flying time from Chicago, IL to Cairo, Egypt. The total flight duration from Chicago, IL to Cairo, Egypt is 12 hours, 47 minutes. This assumes an average flight speed for a commercial airliner of 500 mph, which is equivalent to 805 km/h or 434 knots. It also adds an extra 30 minutes for take-off and landing. Your exact time may vary depending on wind speeds.

Figure 6: A sample relevant document for the MS MARCO FarRelevant collection. The query/question is: "how long is the flight from chicago to cairo". The answer-bearing passage is marked by bold font.

(from 256 to 32,768 tokens), and inserting a single answer-bearing sentence at a random location. An example query-document pair can be found in Figure 4. While this design ensures precise control over document length (doubling per bucket), it introduces several problems:

1. **Extremely low document diversity**: All examples are truncated variants of the same original text, which severely limits the variability in document style and content.
2. **Artificial signal separation**: The inserted answer sentence differs substantially from the background text, making it easy for models to identify it.

The Passkey subset is similar in structure and also uses length-bucketed documents, but instead of a single sentence, it inserts a three-sentence passkey definition into a synthetic background context (see Figure 5). However, the background is even less natural than Needle’s subset background, being composed of unrelated or nonsensical declarative statements (e.g., “The sky is blue. The sun is yellow. Here we go. There and back again.”). This leads to even greater distributional mismatch between signal and context.

Critically, both Needle and Passkey were designed primarily to test *answer extraction* or retrieval of small, highly localized answer-bearing spans. They are not well suited to studying retrieval or ranking of entire passages or documents, especially when relevance is more distributed or contextual.

Our MS MARCO FarRelevant (see Figure 6 for an example) is designed to be textually similar to MS MARCO Documents but with different positional biases for relevant passages. We believe it offers a more robust testbed for long-context *document ranking*. While it is also synthetic in construction, it avoids many of the pitfalls noted above. Each document is created by concatenating multiple passages, which are typically *meaningful* and *complete*, only one of which is relevant to the query. The remaining passages serve as distractors but are independently coherent. Although these documents do not exist in the wild, they are much more diverse in content and style than those in Needle or Passkey despite being typically much shorter. Furthermore, each individual passage is semantically complete and belongs to a real corpus, namely, MS MARCO Passages.

B.4 Positional Bias Identification

To assess positional bias, we used a combination of approximate string matching and LLM-based judging, which was recently shown to highly correlate with human judgments (Upadhyay et al., 2024; Arabzadeh and Clarke, 2025). The resulting distributions can be found in Figure 7.

Approximate string matching was used for MS MARCO training and development (*dev*) sets, both of which have sparse labels. Although initially MS MARCO passages were exact substrings of MS MARCO documents, document and passage texts were collected at different times this lead to some content divergence (Craswell et al., 2021a) that made exact mapping virtually impossible. There have been prior and contemporaneous attempts to recover initial positions, but only with a limited success. In particular, (Coelho et al., 2024) used exact matching and found only about one thousand matching passages. Hofstätter et al. (2020b) used matching of answer words—rather than passage text itself—and were able to match only 32% of the passages. Both of these attempts match only a small-to-modest fraction of passages while being a subject to biases.

Our approximate string matching combines approximate substring matching with longest-substring matching and incorporates efficiency heuristics to identify initial candidate sets. Candidate sets were constructed using two approaches: selecting all relevant passages and documents (for a given query) and retrieving top-5 documents using relevant passages as queries. To assess reliability, we manually inspected a subset of the matched passages and found the procedure to be sufficiently accurate. We then applied this approach to two sets of queries:

- A set of all 5193 queries from the *dev* set;
- A (random and uniform) sample of 5000 training queries.

In both cases, we were able to find matches for about 85% of the queries.

For queries sets with “dense” relevance judgments produced by TREC NIST assessors we used an LLM judge. This included TREC 2019, 2020, 2021 TREC DL queries (Craswell et al., 2021b), Robust04 (Clarke et al., 2004), Gov2 with 2007, 2008 Million Query Track queries (Allan et al., 2008), and ClueWeb12 with 2012 and 2013 Web Track queries (Collins-Thompson et al., 2013b).

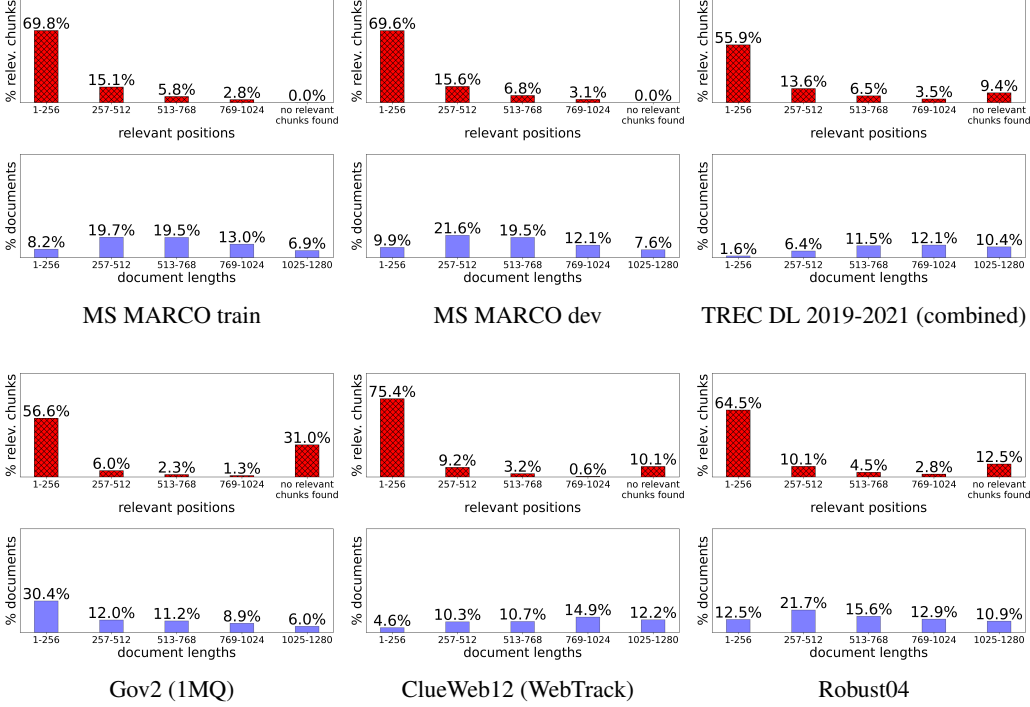


Figure 7: **Illustration of positional relevance bias for three document collections.** We show a distribution of first relevant passage positions (red bars) vs. relevant document lengths (blue bars). Positions and lengths are measured in the number of subword tokens (BERT-base tokenizer). Best viewed in color.

It is noteworthy that Hofstätter et al. (2020b) employed crowd-workers to identify the distribution of relevance chunks. They found similar evidence of the relevance position bias, but their study was limited only to TREC DL 2019 query set.

To avoid potential positional biases in LLM-judging, we divided each document into non-overlapping chunks and judged each chunk separately. Chunking was preserving sentence boundary while ensuring each chunk size was close to having 256 tokens. For efficiency reasons, we only considered at most 36 chunks (about 9K tokens) and 500-2000 positive query-document pairs per query set. A chunk was considered to be relevant if it received a positive grade from the LLM-judge. The LLM-judge model was GPT4-mini (OpenAI, 2023).

For most collections, there was only a small fraction of documents where the LLM-judge found no relevant query-document pairs. One exception is the Gov2 collection with 2007, 2008 Million Query Track queries where this happened in about 30% of the cases. Despite this gap, Gov2 still had a substantial positional bias with about 57% of the cases where the first chunk was deemed to be relevant.

| Model family | # of params. |
|--------------------------------------|-----------------|
| PARADE Transformer | 132-148M |
| Longformer | 149M |
| BigBird | 127M |
| JINA | 137M |
| MOSAIC | 137M |
| DEBERTA-based models | 184M |
| TinyLLAMA-based models | 1034M |
| Other BERT- and ELECTRA-based models | ≈ 110 M |

Table 11: Number of Model Parameters

C Ranking with Cross-Encoding Long-Document Models

In this section, we describe long-document cross-encoding models in more details. With an exception of TinyLLAMA (Zhang et al., 2024) all models use only smallish bi-directional encoder-only Transformers (Vaswani et al., 2017) with 100-200M parameters in total (see Table 11). TinyLLAMA is a so-called LLM-ranker: a “causal” decoder-only Transformer that has about 1B parameters. Moreover, we focus only on the pure-Transformer architectures leaving hybrid architectures such as RankMamba for future work (Xu, 2024).

We assume that an input text is split into small

1712
1713
1714
1715
1716

1717
1718
1719
1720
1721
1722
1723
1724
1725
1726
1727
1728

1729
1730
1731
1732
1733
1734
1735
1736

1737
1738
1739
1740
1741
1742
1743
1744
1745
1746
1747
1748
1749
1750
1751

1752 chunks of texts called *tokens*. Although tokens can
1753 be complete English words, Transformer models
1754 usually split text into sub-word units (Wu et al.,
1755 2016).

1756 The length of a document d —denoted as $|d|$ —
1757 is measured in the number of tokens. Because
1758 neural networks cannot operate directly on text, a
1759 sequence of tokens $t_1 t_2 \dots t_n$ is first converted to
1760 a sequences of d -dimensional embedding vectors
1761 $w_1 w_2 \dots w_n$ by an *embedding* network. These em-
1762 beddings are context-independent, i.e., each token
1763 is always mapped to the same vector (Collobert
1764 et al., 2011; Mikolov et al., 2013).

1765 For a detailed description of Transformer mod-
1766 els, please see the annotated Transformer guide
1767 (Rush, 2018) as well as the recent survey by Lin
1768 et al. (Lin, 2019), which focuses on the use of
1769 BERT-style cross-encoding models for ranking and
1770 retrieval. For this paper, it is necessary to know
1771 only the following basic facts:

- 1772 • BERT is an encoder-only model, which con-
1773 verts a sequence of tokens $t_1 t_2 \dots t_n$ to a se-
1774 quence of d -dimensional vectors $w_1 w_2 \dots w_n$.
1775 These vectors—which are token representa-
1776 tions from the *last* model layer—are com-
1777 monly referred to as contextualized token em-
1778 beddings (Peters et al., 2018);
- 1779 • BERT operates on word pieces (Wu et al.,
1780 2016) rather than on complete words;
- 1781 • The vocabulary includes two special tokens:
1782 [CLS] (an aggregator) and [SEP] (a sepa-
1783 tor);
- 1784 • Using a *pooled* representation of token vectors
1785 $w_1 w_2 \dots w_n$, a linear layer is used to produce
1786 a ranking score. A nearly universal pooling
1787 approach in cross-encoding rankers is to use
1788 the vector of the [CLS] token, i.e., w_1 . How-
1789 ever, we learned that some models (e.g., JINA
1790 (Günther et al., 2023)) converge well *only* with
1791 mean pooling, i.e., they use $\frac{1}{n} \sum_{i=1}^n w_i$.

1792 A “vanilla” BERT ranker (dubbed as monoBERT
1793 by Lin et al. (Lin, 2019)) uses a single fully-connect
1794 layer F as a prediction head, which converts the
1795 last-layer representation of the [CLS] token (i.e., a
1796 contextualized embedding of [CLS]) into a scalar
1797 (Nogueira and Cho, 2019). It makes a prediction
1798 based on the following sequence of tokens: [CLS]
1799 q [SEP] d [SEP], where q is a query and d is a
1800 document.

1801 An alternative approach is to aggregate con-
1802 textualized embeddings of regular tokens using a
1803 shallow neural network (MacAvaney et al., 2019;
1804 Boytsov and Kolter, 2021; Khattab and Zaharia,
1805 2020) (possibly together with the contextualized
1806 embedding of [CLS]). This was first proposed by
1807 MacAvaney et al. (MacAvaney et al., 2019) who
1808 also found that incorporating [CLS] improves per-
1809 formance. However, Boytsov and Kolter proposed
1810 a shallow aggregating network that does not use the
1811 output of the [CLS] token and achieved the same
1812 accuracy on MS MARCO datasets (Boytsov and
1813 Kolter, 2021).

1814 Replacing the standard BERT model in the
1815 vanilla BERT ranker with a BERT variant that “na-
1816 tively” supports longer documents (e.g., Big-Bird
1817 (Zaheer et al., 2020)) is, perhaps, the simplest way
1818 to deal with long documents. We collectively call
1819 these models as LongP models. For a typical BERT
1820 model, however, long documents and queries need
1821 to be split or truncated so that the overall num-
1822 ber of tokens does not exceed 512. In the *FirstP*
1823 mode, we process only the first chunk and ignore
1824 the truncated text. In the *SplitP* mode, each chunk
1825 is processed separately and the results are aggre-
1826 gated. In the remaining of this section, we discuss
1827 these approaches in detail.

C.1 LongP models

1828 In our work, we benchmark both sparse-attention
1829 and full-attention models. Sparse attention LongP
1830 models include two popular options: Longformer
1831 (Beltagy et al., 2020) and Big-Bird (Zaheer et al.,
1832 2020). In that, we use the same approach to
1833 score documents as with the vanilla BERT ranker,
1834 namely, concatenating queries with documents and
1835 making a prediction based on the contextualized
1836 embedding of the [CLS] token (Nogueira and Cho,
1837 2019). Both Big-Bird and Longformer use a com-
1838 bination of the local, “scattered” (our terminol-
1839 ogy), and global attention. The local attention utilizes a
1840 sliding window of a constant length where each to-
1841 ken attends to each other token within this window.
1842 In the case of the global attention, certain tokens
1843 can attend to *all* other tokens and vice-versa. In
1844 Big-Bird, only special tokens such as [CLS] can
1845 attend globally. In Longformer, the user have to
1846 select such tokens explicitly. Following Beltagy
1847 et al. (Beltagy et al., 2020), who applied this tech-
1848 nique to question-answering, we “place” global
1849 attention only on query tokens. Unlike the global

attention, the scattered attention is limited to restricted sub-sets of tokens, but these subsets do not necessarily have locality. In Big-Bird the scattered attention relies on random tokens, whereas Longformer uses a dilated sliding-window attention with layer- and head-specific dilation.

Full-attention models include JINABert (Günther et al., 2023), TinyLLAMA (Zhang et al., 2024), and MosaicBERT (Portes et al., 2023), henceforth, simply JINA, TinyLLAMA and MOSAIC. All these models use a recently proposed FlashAttention (Dao et al., 2022) to efficiently process long-contexts as well as special positional embeddings that can generalize to document lengths not seen during training. In that, JINA and MOSAIC use AliBi (Press et al., 2022), while TinyLLAM uses ROPE embeddings (Su et al., 2023). JINA and MOSAIC are bi-directional encoder-only Transformer model whereas TinyLLAMA is a unidirectional (sometimes called causal) decoder-only Transformer model (Vaswani et al., 2017).

In addition architectural difference, models differ in pretraining strategies. MOSAIC relies primarily on the masked language (MLM) objective without next sentence prediction (NSP). JINA uses this approach as a first step, following a RoBERTa pretraining strategy (Liu et al., 2019) and fine-tuning on retrieval and classification tasks with mean-pooled representations. TinyLLAMA was trained using an autoregressive language modeling objective (Zhang et al., 2024). We found that JINA lost an ability to effectively pool on the [CLS] token and we used mean-pooling instead. We also use mean pooling for TinyLLAMA. For MOSAIC we used pooling on [CLS].

C.2 SplitP models

SplitP models differ in partitioning and aggregation approaches. Documents can be split into either disjoint or overlapping chunks. In the first case, documents are split in a greedy fashion so that each document chunk except possibly the last one is exactly 512 tokens long after being concatenated with a (padded) query and three special tokens. In the second case, we use a sliding window approach with a window size and stride that are not tied to the maximum length of BERT input. Because our primary focus is accuracy and we aim to understand the limits of long-document models, we exclude from evaluation several *SplitP* models, e.g., by Hofstätter et al. (2021b); Zou et al. (2021),

which achieve better efficiency-effectiveness trade-offs by pre-selecting certain document parts and feeding only selected parts into a BERT ranker.

Greedy partitioning into disjoint chunks CEDR models (MacAvaney et al., 2019) and the Neural Model 1 (Boytsov and Kolter, 2021) use the first method, which involves:

- tokenizing the document d ;
- greedily splitting a tokenized document d into m disjoint chunks: $d = d_1 d_2 \dots d_m$;
- generating m token sequences [CLS] q [SEP] d_i [SEP] by concatenating the query with document chunks;
- processing each sequence with a BERT model to generate contextualized embeddings for regular tokens as well as for [CLS].

The outcome of this procedure is m [CLS]-vectors cls_i and n contextualized vectors $w_1 w_2 \dots w_n$ (one for *each* document token t_i) that are aggregated in a model-specific ways.

MacAvaney et al. (MacAvaney et al., 2019) use contextualized embeddings as a direct replacement of context-free embeddings in the following neural architectures: KNRM (Xiong et al., 2017), PACRR (Hui et al., 2018), and DRMM (Guo et al., 2016). To boost performance, they incorporate [CLS]-vectors in a model-specific way. We call the respective models as *CEDR-KNRM*, *CEDR-PACRR*, and *CEDR-DRMM*.

They also proposed an extension of the vanilla BERT ranker that makes a prediction using the average [CLS] token: $\frac{1}{m} \sum_{i=1}^m cls_i$ by passing it through a linear projection layer. We call this method *AvgP*.

The Neural Model 1 (Boytsov and Kolter, 2021) uses the same greedy partitioning approach as CEDR, but a different aggregator network, which does not use the embeddings of the [CLS] token. This network is a neural parametrization of the classic Model 1 (Berger and Lafferty, 1999; Brown et al., 1993).

Sliding window approach The BERT MaxP/SumP (Dai and Callan, 2019) and PARADE (Li et al., 2024) models use a sliding window approach. Assume w is the size of the window and s is the stride. Then the processing can be summarized as follows:

- tokenizing, the document d into sub-words $t_1 t_2 \dots t_n$;
- splitting a tokenized document d into m possibly overlapping chunks $d_i = t_{i \cdot s} t_{i \cdot s+1} \dots t_{i \cdot s+w-1}$: Trailing chunks may have fewer than w tokens.
- generating m token sequences [CLS] q [SEP] d_i [SEP] by concatenating the query with document chunks;
- processing each sequence with a BERT model to generate a last-layer output for each sequence [CLS] token.

The outcome of this procedure is m [CLS]-vectors cls_i , which are subsequently aggregated in a model-specific ways. Note that PARADE and MaxP/SumP models do not use contextualized embeddings of regular tokens.

BERT MaxP/SumP These models (Dai and Callan, 2019) use a linear layer F to produce m relevance scores $F(cls_i)$. Then complete document scores are computed as $\max_{i=1}^m F(cls_i)$ and $\sum_{i=1}^m F(cls_i)$ for the MaxP and SumP models, respectively.

PARADE These models (Li et al., 2024) can be divided into two groups. The first group includes PARADE average, PARADE max, and PARADE attention, which all use simple approaches to produce an aggregated representation of m [CLS]-vectors cls_i . To compute a relevance score these aggregated representations are passed through a linear layer F .

In particular, PARADE average and PARADE max combine cls_i using averaging and the element-wise maximum operation, respectively to generate aggregated representation of m [CLS] tokens cls_i .¹⁰ The PARADE attention model uses a learnable attention (Bahdanau et al., 2015) vector C to compute a scalar weight w_i of each i as follows: $w_1 w_2 \dots w_m = \text{softmax}(C \cdot cls_1, C \cdot cls_2, \dots, C \cdot cls_m)$. These weights are used to compute the aggregated representation as $\sum_{i=1}^m w_i cls_i$

¹⁰Note that both PARADE average and AvgP vanilla ranker use the same approach to aggregate contextualized embeddings of [CLS] tokens, but they differ in their approach to select document chunks. In particular, AvgP uses non-overlapping chunks while PARADE average relies on the sliding window approach.

PARADE Transformer models combine [CLS]-vectors cls_i with an additional *aggregator* transformer model $\text{AggregTransf}()$. The input of the aggregator Transformer is sequence of cls_i vectors prepended with a learnable vector C , which plays a role of a [CLS] embedding for $\text{AggregTransf}()$. The last-layer representation of the first vector is passed through a linear layer F to produce a relevance score:

$$F(\text{AggregTransf}(C, cls_1, cls_2, \dots, cls_m)[0]) \quad (1)$$

An aggregator Transformer can be either pre-trained or randomly initialized. In the case of a pretrained transformer, we completely discard the embedding layer. Furthermore, if the dimensionality of cls_i vectors is different from the dimensionality of input embeddings in AggregTransf , we project cls_i using a linear transformation.

Miscellaneous models We attempted to implement additional state-of-the-art models (Gao and Callan, 2022; Fu et al., 2022). Gao and Callan (Gao and Callan, 2022) introduced a late-interaction model MORES+, which is a modular long document reranker that uses a sequence-to-sequence transformer in a non-auto-regressive mode. In MORES+ document chunks are first encoded using the encoder-only Transformer model. Then they use a modified decoder Transformer for joint query-to-all-document-chunk cross-attention: This modification changes a causal Transformer into an encoder-only bi-directional Transformer model. As of the moment of writing, the MORES+ model holds the first position on a competitive MS MARCO document leaderboard.¹¹. However, the authors provide only incomplete implementation which does not fully match the description in the paper (i.e., crucial details are missing). We reimplemented this model to the best of our understanding, but our implementation failed to outperform even BM25.

Inspired by this approach, we managed to implement a late-interaction variant of the PARADE model, which we denoted as PARADE-LATEIR. Similar to the original PARADE model, it splits documents into overlapping chunks. However, it then encodes chunks and queries independently. Next, it uses an interaction Transformer to (1) mix these representations, and (2) combine output using

¹¹<https://microsoft.github.io/MSMARCO-Document-Ranking-Submissions/leaderboard/>

2036 an aggregator Transformer. In total, the model uses
2037 three backbone encoder-only Transformers: All of
2038 these Transformers are initialized using pretrained
2039 models.

2040 [Fu et al. \(2022\)](#) proposed a multi-view
2041 interactions-based ranking model (MIR). They im-
2042 plement inter-passage interactions via a multi-view
2043 attention mechanism, which enables information
2044 propagation at token, sentence, and passage levels.
2045 Due to the computational complexity, they restrict
2046 these interactions to a set of salient/pivot tokens.
2047 However, the paper does not provide enough de-
2048 tails regarding the choices of these tokens. There is
2049 no software available and authors did not respond
2050 to our clarification requests. Thus, this model is
2051 also excluded from our evaluation.